Power Adaptive Network Coding for a Non-Orthogonal Multiple-Access Relay Channel

Sha Wei, Jun Li, *Member, IEEE*, Wen Chen, *Senior Member, IEEE*, Hang Su, Zihuai Lin, *Senior Member, IEEE*, and Branka Vucetic, *Fellow, IEEE*

***Abstract*—In this paper we propose a novel power adaptive network coding (PANC) for a non-orthogonal multiple-access relay channel (MARC), where two sources transmit their information simultaneously to the destination with the help of a relay. In contrast to the conventional XOR-based network coding (CXNC), the relay in PANC generates network coded symbols by considering the coefficients of the source-to-relay channels, and forwards each symbol with a pre-optimized power level. Specifically, by defining a symbol pair as two symbols from the two sources, we first derive the expression of symbol pair error rate (SPER) for the system. Noting that deriving the exact SPER are complex due to the irregularity of the decision regions caused by random channel coefficients, we propose a coordinate transform (CT) method on the received constellation to simplify the derivations of the SPER. Next, we obtain the optimal power level by decomposing it as a multiplication of a power scaling factor and a power adaptation factor. We prove that with the power scaling factor at the relay, our PANC scheme can achieve a full diversity gain, i.e., an order of two diversity gain, while the CXNC can achieve only an order of one diversity gain. In addition, we optimize the power adaptation factor at the relay to minimize the SPER at the destination by considering of the relationship between SPER and minimum Euclidean distance of the received constellation, resulting in an improved coding gain. Simulation results show that (1) the SPER derived based on our CT method can well approximate the exact SPER with a much lower complexity; (2) the PANC scheme with power adaptation optimizations and power scaling factor design can achieve a full diversity, and obtain a much higher coding gain than other network coding schemes.**

***Index Terms*—Network coding, power optimization, multiple access relay channel, error probability.**

I. Introduction

RELAYING techniques have been considered for decades as a method to improve the reliability of wireless networks by exploiting spatial diversity via intermediate relay nodes [1, 2]. Network coding, on the other hand, originated from wire-line networks [3, 4], has been recently applied to wireless networks to enhance the network throughput [5]. With the implementations of diversity techniques and network coding at the relay nodes, it is anticipated that wireless networks can achieve reliable and high throughput communications.

There are two typical network models which are suitable for the applications of network coding, namely, two-way relay channel (TWRC) and multiple access relay channel (MARC). In the TWRC, the two sources want to exchange information with each other with the assistance of a relay. Since each source perfectly knows its own information, it can easily remove its own information from the received network coded signal. Compared with the convectional transmission schemes without network coding in the TWRC, network coding can enhance the throughput by taking the advantage of the multi-user interference [6–9]. That is, we can reduce the transmission time slots by generating network coded signal from the interfered received signal at the relay. In [6], an optimal network coded relay function [10] is derived to minimize the bit error rate in the TWRC. In [7], physical-layer network coding is proposed, where the relay maps the interfered signals from the two sources to a network coded digit. In [8], denoise-and-forward based network coding schemes are designed for the TWRC with multi-user interferences.

On the other hand, MARC has been recognized as a fundamental building block for cellular and wireless sensor networks. The MARC is a model for network topologies where multiple sources communicate with a single destination in the presence of a relay. A typical example is in a cellular systems where two mobile users communicate with a base station with the help of a relay. Different from the TWRC, the MARC only has imperfect information at the destination from the sources. Currently, there are a number of interesting research on network coding design in the MARC. In [11–17], the authors consider the orthogonal MARC systems, and multi-user interference is not considered, which leads to a low spectrum efficiency. In [18], a non-orthogonal MARC is studied with additive white Gaussian noise (AWGN) channels. Therefore, channel fading and diversity gain are not considered. In [19], the authors consider an orthogonal MARC, where the sources transmit information to a sink through the assistance of a relay. Also, the authors analyze the union bound of the bit error probability, which is sufficient to obtain the diversity performance of the system. However, it is not accurate enough to derive the optimal system parameters, which maximize the coding gain. In [20], the authors study both the orthogonal and non-orthogonal MARC. Particularly in the non-orthogonal MARC,

Manuscript received April 24, 2013; revised September 25 and December 17, 2013. The editor coordinating the review of this paper and approving it for publication was M. Xiao.

S. Wei, W. Chen, and H. Su are with the Department of Electronic Engineering, Shanghai Jiaotong University, Shanghai, China, 200240 (e-mail: {venessa724, wenchen, Hmilyanjohn}@sjtu.edu.cn).

J. Li, Z. Lin, and B. Vucetic are with the School of Electrical and Information Engineering, The University of Sydney, NSW, 2006, Australia {jun.li1, zihuai.lin, branka.vucetic}@sydney.edu.au).

This work is supported by the National 973 Project #2012CB316106, by NSF China #61161130529 and #61328101, by the STCSM Science and Technology Innovation Program #13510711200, by the SEU National Key Lab on Mobile Communications #2013D11, and by the Australian Research Council (ARC) Project LP110100110 with ZTE for financial support.

Digital Object Identifier 10.1109/TCOMM.2014.013114.130303

the authors address the issue of the multi-user interference, and propose a network coded selective-and-forward relaying scheme to achieve full diversity gain by dropping erroneous messages. In [21], the authors design a compute-and-forward network coding coefficients by Fincke-Pohst based candidate set searching algorithm and network coding system matrix constructing algorithm to maximize the transmission rate in a multi-source multi-relay system.

In this paper, we are interested in designing novel network coding schemes for a non-orthogonal MARC over fading channels to achieve a full diversity gain and a high coding gain. Although by dropping erroneous source-relay symbols, finite-field network coding (FFNC) has been shown to achieve a full diversity in both orthogonal and non-orthogonal MARC [20], some useful information is also discarded in the process which may lead to the loss of coding gain. Also, we will prove that conventional XOR-based network coding (CXNC)[1] without any error propagation mitigation process at relay cannot achieve full diversity gain in a non-orthogonal MARC due to multi-user interference. Specifically in this paper, we consider a two-source, one-relay, one destination non-orthogonal MARC.

There are three major concerns in our network coding design. Firstly, we consider how to achieve the full diversity gain of the MARC. We propose a novel power adaptation network coding (PANC) scheme to achieve the full diversity gain, in which the power level is the multiplication of a power scaling factor and a power adaptation factor with two levels. In contract to the CXNC, the relay in the proposed PANC generates network coded symbols by considering the coefficients of the global channels, and forwards each symbol with one of the two given power levels. Specifically, based on the received signals, the relay decides which power level should be applied to each network coded symbol. We prove that the PANC scheme with the design of power scaling at the relay can achieve a full diversity gain, i.e., a diversity of two, while the CXNC scheme can achieve only a diversity of one. Different from the relay scheme proposed in our earlier work [22], in order to adapt the real-number modulation at sources, the relay transmits a real number in PANC scheme instead of a complex lattice code proposed in [22]. However, these two works share the same insight that CXNC with or without any error propagation mitigation techniques at relay cannot achieve full diversity. Also, in our previous work, we did not consider design of mitigating error propagation from source-relay hop to destination, and we did not analyze the diversity order of the system.

Secondly, we consider how to evaluate the error performance of the system. By defining a symbol pair as two symbols from the two sources, we develop the expression of symbol pair error rate (SPER), with the received constellations at both the relay and the destination. Due to the irregularity of the decision regions on the received constellation, we adopt the wedge probability computation method [23] to investigate the SPER. Noting that the derivations of the exact SPER based on original received constellation are complicated, we further propose a coordinate transform (CT) method to simplify the derivations. In the CT method, we transform the original parallelogram geometry to a rectangle one and approximate the exact expressions based on the original constellation with simpler SPER expressions.

Thirdly, we consider how to achieve a high coding gain. We will minimize the SPER by optimizing the two power adaptation levels. Specifically, we propose a criteria based on the relationship between the Euclidean distance and the SPER, and formulate a convex optimization problem to develop the optimal power adaptation levels at the relay.

Based on the above discussions, there are four main contributions of this paper as follows. (a) We propose a novel PANC scheme with a power scaling design at the relay to achieve full diversity. (b) We propose a CT method to transform the parallelogram-shaped constellation to a rectangle one, which simplify the SPER derivation. (c) We further derive the approximate SPER based on the transformed constellation. (d) We optimize the power adaptation at the relay to achieve a higher coding gain.

Simulation results show that (a) the derived SPER based on our CT method can well approximate the exact SPER with a much lower complexity, (b) the PANC scheme with power adaptation level optimizations and power scaling factor design can achieve a full diversity and obtain a much higher coding gain than the PANC scheme with randomly chosen power levels, and (c) the CXNC scheme cannot achieve a full diversity with or without the power scaling design.

The rest of this paper is organized as follows. We first describe the system model in Section II and propose the PANC scheme in Section III. Then we develop the exact system SPER and its approximation in Section IV. In Section V, we address the error propagation problem, and formulate and solve the optimization problem by minimizing the system SPER. Simulation results are summarized in Section VI, and conclusions are given in Section VII.

The notations used in this paper are as follows. We denote a ray by l_{ij} where the subscript ij is the label of the line. A line segment is denoted by AB, and $\overline{AB}$ denotes the length between points A and B. We use the terms *ray-vertex-ray* and *ray-vertex-vertex-ray* to describe a wedge and wedge combination, respectively. The one-dimensional Q-function is defined as $Q_1(x) = \frac{1}{\pi}\int_0^{\frac{\pi}{2}} \exp\left(-\frac{x^2}{2\sin^2\theta}\right) d\theta$. The notation for a two-dimensional Q-function $Q_2(x, y; \rho)$ with $x = y$ is simplified as $Q_2(x;\rho) = \frac{1}{\pi}\int_0^{\arctan\left(\sqrt{\frac{1+\rho}{1-\rho}}\right)} \exp\left(-\frac{x^2}{2\sin^2\phi}\right) d\phi$.

II. System Model

Consider a two-source single-relay multiple-access relaying system, where two sources $\mathcal{S}_1$ and $\mathcal{S}_2$ transmit their information to the common destination $\mathcal{D}$ with the assistance of a half-duplex relay $\mathcal{R}$. Each transmission period is divided into two transmission phases. In a symbol time slot of the first transmission phase, the two sources simultaneously broadcast their symbols x_1 and x_2 to both the destination and the relay. In a symbol time slot of the second transmission phase, the two sources keep silent, while the relay processes the received signals and forwards the network coded symbol $x_{\mathcal{R}}$ to the

[1]If not particularly indicated, the CXNC scheme in this paper does not detect and drop erroneous symbols at the relay.

destination. At the end of the second phase, the destination decodes the two sources' information based on the received signals.

We assume that all the transmitted signals are BPSK modulated with equal probability, i.e., $x_1, x_2, x_{\mathcal{R}} \in \{\pm 1\}$, and all the signals are transmitted in the same frequency band. The channel between any two given nodes j and k, $j \in \{1, 2, \mathcal{R}\}, k \in \{\mathcal{R}, \mathcal{D}\}$, and $j \neq k$, is denoted by h_{jk} with a subscript indicating the nodes under consideration. We assume that h_{jk} for all the j and k are Rayleigh distributed with a mean zero and variance $\bar{\gamma}_{jk}$. We consider slow fading channels in our system, i.e., the channel coefficients are constant during a transmission period, while they change independently from one transmission period to another.

Also, we implement the channel phase pre-equalization for both the source-to-destination multiple access channels (MAC) and the relay-to-destination channel before each transmission. Thus, the effective source-to-destination and relay-to-destination channel coefficients can be regarded as real-valued channels, i.e., real channel coefficients and real values of noise samples. The carrier phase synchronization is practical by adopting methods shown in [24] [25]. Note that, without the phase synchronization assumption, the wedge error probability method is not applicable to analyze SPER. Therefore, the closed-form of the optimal power levels κ_1 and κ_2 cannot be achieved.

Based on the aforementioned system settings and assumptions, the received signals at the relay and destination in the first transmission phase can be written as

$$\begin{aligned} y_{\mathcal{R}} &= \sqrt{E_1} h_{1\mathcal{R}} x_1 + \sqrt{E_2} h_{2\mathcal{R}} x_2 + n_{\mathcal{R}}, \\ y_1 &= \sqrt{E_1} |h_{1\mathcal{D}}| x_1 + \sqrt{E_2} |h_{2\mathcal{D}}| x_2 + n_1, \end{aligned} \tag{1}$$

respectively, where E_1 and E_2 denote the transmission power of $\mathcal{S}_1$, $\mathcal{S}_2$, respectively, $n_{\mathcal{R}}$ is a complex additive white Gaussian noise (AWGN) sample at the relay with a zero mean and variance $\sigma^2/2$ per dimension, and n_1 is a real AWGN sample at the destination with zero mean and variance σ^2.

As we adopt the joint power scaling and adaptation scheme at the relay, the instantaneous power at the relay is optimized given the channel realization within each transmission period with the aim to minimize the SPER and achieve a full diversity at the destination. Specifically, in the power scaling, we have the scaling factor α ($0 \leq \alpha \leq 1$) which is determined based on the channel conditions. In the power adaptation, we have two power levels, namely, $\tilde{\kappa}_1$ and $\tilde{\kappa}_2$, related as $\tilde{\kappa}_1^2 + \tilde{\kappa}_2^2 \leq 2E_{\mathcal{R}}^{\text{ave}}$, where $E_{\mathcal{R}}^{\text{ave}}$ denotes the relay average transmission power. The calculations of $\alpha, \tilde{\kappa}_1, \tilde{\kappa}_2$ will be discussed later. Therefore, in the second transmission phase, the received signal at destination can be expressed as

$$y_2 = \sqrt{E_{\mathcal{R}}} |h_{\mathcal{R}\mathcal{D}}| x_{\mathcal{R}} + n_2, \tag{2}$$

where n_2 is a real AWGN sample at destination with a zero mean and variance σ^2, and $E_{\mathcal{R}} \in \{\kappa_1, \kappa_2\}$ represents the transmission power at relay with $\kappa_i = \alpha \tilde{\kappa}_i$ for $i \in \{1, 2\}$. In this paper, we have the following assumption of instantaneous CSIs. In order to realize channel phase pre-equalization, the instantaneous CSIs available at source are $h_{1\mathcal{D}}$, $h_{2\mathcal{D}}$ and $h_{\mathcal{R}\mathcal{D}}$. In addition, to compute the scaling factor α, the instantaneous CSIs available at relay are $h_{1\mathcal{R}}$, $h_{2\mathcal{R}}$ and $h_{\mathcal{R}\mathcal{D}}$ (or statistical CSI $\gamma_{\mathcal{R}\mathcal{D}}$). Moreover, to obtain the transmission power (κ_1, κ_2) and joint ML detection at destination, the instantaneous CSIs available at destination are $h_{1\mathcal{D}}$, $h_{2\mathcal{D}}$, $h_{1\mathcal{R}}$, $h_{2\mathcal{R}}$, and $h_{\mathcal{R}\mathcal{D}}$.

III. Network Coded Power Adaptation Scheme at the Relay

In the conventional network coding based MARC, XOR operations are implemented at the relay on the two sources' information. We will show later in Section V that the system cannot achieve a full diversity with the conventional network coding. To achieve a full diversity, we propose the PANC scheme, i.e., based on the received signals, the relay transmits a network coded symbol multiplied with an optimized power level.

Firstly, the relay obtain the two sources' message symbols (x_1, x_2) from its received signal $y_{\mathcal{R}}$ by utilizing the maximum likelihood (ML) detection, i.e.,

$$(\hat{x}_1, \hat{x}_2) = \underset{\tilde{x}_1, \tilde{x}_2 \in \{\pm 1\}}{\arg\min} \left| y_{\mathcal{R}} - \sqrt{E_{1\mathcal{R}}} h_{1\mathcal{R}} \tilde{x}_1 - \sqrt{E_{2\mathcal{R}}} h_{2\mathcal{R}} \tilde{x}_2 \right|^2, \tag{3}$$

where $(\hat{\cdot})$ denotes the detected symbol, and $(\tilde{\cdot})$ denotes the trial symbol used in the hypothesis-detection problem. Then the relay performs a network coding operation on the two detected symbols. The network coded operation in our PANC [2] is denoted by $\boxplus$, which is different from the conventional XOR operation. That is, we calculate $x_{\mathcal{R}}$ by $x_{\mathcal{R}} = \hat{x}_1 \boxplus \hat{x}_2 = \text{sign}(|h_{1\mathcal{R}}|\hat{x}_1 + |h_{2\mathcal{R}}|\hat{x}_2)$. Next, the relay chooses the power level $E_{\mathcal{R}}$ based on the decoded symbols, i.e., if $(\hat{x}_1 = 1, \hat{x}_2 = 1)$ or $(\hat{x}_1 = -1, \hat{x}_2 = -1)$, power level is chosen as κ_1; else if $(\hat{x}_1 = 1, \hat{x}_2 = -1)$ or $(\hat{x}_1 = -1, \hat{x}_2 = 1)$, power level is chosen as κ_2. The reason for adopting the new proposed network coding operation and power level allocation method is that the received constellation at destination is a parallelogram, on which the $(\hat{x}_1 = 1, \hat{x}_2 = 1)$ corresponding constellation point lies in a diagonal with the $(\hat{x}_1 = -1, \hat{x}_2 = -1)$ corresponding constellation point. While for XOR operation, the received constellation is an irregular quadrilateral no matter what power level allocation result we implement.

The values of κ_1 and κ_2 are optimized by obtaining the power scaling factor α, and the optimal power adaptation factors $\tilde{\kappa}_1$ and $\tilde{\kappa}_2$, respectively. For the power scaling factor, the relay considers the relative values of channel gains of source-relay channel and relay-destination gains. Let us assume that the instantaneous channel state information (CSI) is available to the destination before the transmission period starts. Then, for the power adaptation factors, the destination optimizes $\tilde{\kappa}_1$ and $\tilde{\kappa}_2$ by minimizing the instantaneous SPER based on the CSI, and then feedbacks the values to the relay before the transmission period starts. The relay will use the optimal power level, which is the multiplication of the power scaling factor and the power adaptation factor, to transmit the network

[2] Although the proposed PANC strategy shares some similarities compared with DF strategy with a 4-PAM modulation, it is essentially different from such scheme since the power levels κ_1 and κ_2 are not fixed in different system settings like 4-PAM modulation. They are optimized at destination according to instantaneous CSI, and feedback to relay to achieve a better error performance.

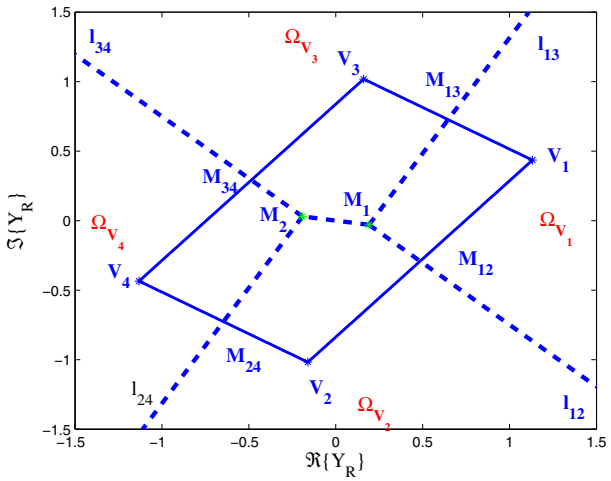

Fig. 1. One possible instantaneous relay constellation, where dashed lines represent boundaries of decision regions.

coded symbol $x_{\mathcal{R}}$. Note that, as the values of $\tilde{\kappa}_1$ and $\tilde{\kappa}_2$ are derived based on the instantaneous CSI, their values will keep invariant within each transmission period, and change from one transmission period to another. The detailed derivation of both the power scaling factor and power adaptation factors will be discussed in Section V.

The PANC scheme at the relay can also be illustrated by a two-dimensional instantaneous relay constellation (IRC), which is associated with the SPER calculation in the next section. The signal part of $y_{\mathcal{R}}$, i.e., $\sqrt{E_1}h_{1\mathcal{R}}x_1+\sqrt{E_2}h_{2\mathcal{R}}x_2$, can be seen as a point in the IRC with X-axis being its real part, and Y-axis being its imaginary part. We define the constellation points (CPs) V_i of the IRC, $i = 1,\cdots,4$, to represent the four possible values of $\pm\sqrt{E_1}h_{1\mathcal{R}} \pm \sqrt{E_2}h_{2\mathcal{R}}$, and define the sources' symbol pairs by $T_i \triangleq (x_1, x_2)$. Specifically, we have $T_1 \triangleq (1,1), T_2 \triangleq (-1,1), T_3 \triangleq (1,-1)$, and $T_4 \triangleq (-1,-1)$.

From Fig. 1, we can see that the geometry of the IRC composed by CPs, denoted by V_i, is a parallelogram. Similar to the Voronoi diagram in [26], the decision regions are segmented by the perpendicular bisectors of each side of the parallelogram. Specifically, rays l_{12}, l_{13}, l_{24} and l_{34} are perpendicular bisectors of sides V_1V_2, V_1V_3, V_2V_4 and V_3V_4, respectively, M_1 is the crossing point of rays l_{12} and l_{13}, and M_2 is the crossing point of rays l_{24} and l_{34}. M_{ij} is the middle point of a side V_iV_j. The decision region Ω_{V_1} of V_1, defined as wedge $l_{12} - M_1 - l_{13}$ in Fig 1, and is given by

$$\begin{aligned}\Omega_{V_1} \triangleq \Bigg\{ & \frac{\Re\{h_{2\mathcal{R}}\}}{\Im\{h_{2\mathcal{R}}\}}\Re\{y_{\mathcal{R}}\} + \Im\{y_{\mathcal{R}}\} - \Im\{h_{1\mathcal{R}}\} \\ & - \frac{\sqrt{E_1}\Re\{h_{1\mathcal{R}}\}\Re\{h_{2\mathcal{R}}\}}{\Im\{h_{2\mathcal{R}}\}} < 0 \text{ and} \\ & \frac{\Re\{h_{1\mathcal{R}}\}}{\Im\{h_{1\mathcal{R}}\}}\Re\{y_{\mathcal{R}}\} + \Im\{y_{\mathcal{R}}\} - \Im\{h_{2\mathcal{R}}\} \\ & - \frac{\sqrt{E_2}\Re\{h_{1\mathcal{R}}\}\Re\{h_{2\mathcal{R}}\}}{\Im\{h_{1\mathcal{R}}\}} \geq 0 \Bigg\}.\end{aligned} \tag{4}$$

Similarly, we can obtain the decision regions of V_2, V_3 and V_4, denoted by Ω_{V_2}, Ω_{V_3}, and Ω_{V_4}, respectively. Based on the four decision regions, we have the one-to-one mapping between the CPs and the network coded power level as

$$\sqrt{E_{\mathcal{R}}}x_{\mathcal{R}} = \begin{cases} \kappa_1 & \text{if } (\Re\{y_{\mathcal{R}}\}, \Im\{y_{\mathcal{R}}\}) \in \Omega_{V_1}, \\ \kappa_2 & \text{if } (\Re\{y_{\mathcal{R}}\}, \Im\{y_{\mathcal{R}}\}) \in \Omega_{V_2}, \\ -\kappa_2 & \text{if } (\Re\{y_{\mathcal{R}}\}, \Im\{y_{\mathcal{R}}\}) \in \Omega_{V_3}, \\ -\kappa_1 & \text{if } (\Re\{y_{\mathcal{R}}\}, \Im\{y_{\mathcal{R}}\}) \in \Omega_{V_4}, \end{cases} \tag{5}$$

Based on the observations y_1 and y_2, the destination jointly decode the two source symbols with the minimum Euclidean distance detection. Then we have

$$\begin{aligned}(\hat{x}_1, \hat{x}_2) = \underset{\tilde{x}_1,\tilde{x}_2\in\{\pm 1\}}{\arg\min} \Bigg(& \left| y_1 - \sum_{j=1}^{2} |h_{j\mathcal{D}}|\tilde{x}_j \right|^2 \\ & + \left| y_2 - |h_{\mathcal{R}\mathcal{D}}|\sqrt{\tilde{E}_{\mathcal{R}}}\,(\tilde{x}_1 \boxplus \tilde{x}_2) \right|^2 \Bigg),\end{aligned} \tag{6}$$

where $\tilde{E}_{\mathcal{R}} \in \{\kappa_1, \kappa_2\}$ is determined by $\tilde{x}_1$ and $\tilde{x}_2$.

IV. Error Performance Analysis

In this section, we investigate the instantaneous SPER performance of the PANC given a channel realization vector $\mathbf{h} = [h_{1\mathcal{R}}, h_{2\mathcal{R}}, h_{1\mathcal{D}}, h_{2\mathcal{D}}, h_{\mathcal{R}\mathcal{D}}]$. Assuming that symbols are transmitted with equal probability, then the general expression of the system SPER of the PANC scheme is

$$P_{e,inst} = \sum_{i=1}^{4} P(\mathcal{E}|T_i, \mathbf{h})P(T_i) = \frac{1}{4}\sum_{i=1}^{4} P(\mathcal{E}|T_i, \mathbf{h}), \tag{7}$$

where T_i is the symbol pair defined in Section III, $\mathcal{E}$ denotes the symbol error event at the destination that a transmitted symbol pair from two sources is decoded to an erroneous pair, i.e., either x_1 or x_2 is wrongly detected or both x_1 and x_2 are wrongly detected, $P(\mathcal{E}|T_i, \mathbf{h})$ is the conditional SPER given T_i is transmitted and the channel realization $\mathbf{h}$, and $P(T_i) = \frac{1}{4}$ is the probability that T_i is sent by the two sources. Since the decision regions of T_1 and T_4 are symmetric, and the decision regions of T_2 and T_3 are symmetric, we have $P(\mathcal{E}|T_1) = P(\mathcal{E}|T_4)$ and $P(\mathcal{E}|T_2) = P(\mathcal{E}|T_3)$. Therefore, (7) can be rewritten as

$$\begin{aligned}P_{e,inst} &= \frac{1}{2}\left(P(\mathcal{E}|T_1, \mathbf{h}) + P(\mathcal{E}|T_2, \mathbf{h})\right) \\ &= \frac{1}{2}\Bigg\{\sum_{i=1}^{2}\sum_{k\in\{\pm a,\pm b\}} P(\mathcal{E}|k, T_i, h_{1\mathcal{D}}, h_{2\mathcal{D}}, h_{\mathcal{R}\mathcal{D}}) \\ &\quad P(\sqrt{E_{\mathcal{R}}}x_{\mathcal{R}} = k|T_i, h_{1\mathcal{R}}, h_{2\mathcal{R}})\Bigg\},\end{aligned} \tag{8}$$

where $P(\sqrt{E_{\mathcal{R}}}x_{\mathcal{R}} = k|T_i, h_{1\mathcal{R}}, h_{2\mathcal{R}})$ is the conditional probability that $x_{\mathcal{R}}$ is allocated to the power level $|k|$ at the relay, and $P(\mathcal{E}|k, T_i, h_{1\mathcal{D}}, h_{2\mathcal{D}}, h_{\mathcal{R}\mathcal{D}})$ is the conditional probability that the destination makes a wrong decision on the sources' symbol pair T_i. For the sake of simplicity, we omit the channel coefficients in these notations, and use $P(\sqrt{E_{\mathcal{R}}}x_{\mathcal{R}} = k|T_i)$ and $P(\mathcal{E}|k, T_i)$.

Since deriving the exact instantaneous SPER of the system requires complicated computation and is time-consuming, in the following, we will derive $P_{e,inst}$ based on a coordinate transformed constellation with a small accuracy loss. Due to the randomness of channel realizations, the two-dimension

decision regions of a symbol pair T_i at both the relay and the destination are irregular and wedge-like, e.g., one possible case of the received constellation and its corresponding decision regions at the relay is shown in Fig. 1. Although the SPER result is accurate with original IRC, the calculations of the SPER could be very complicated. Here, we will propose a coordinate transformation method to derive the SPER, which reduces the calculation complexity with a small sacrifice in accuracy in the low SNR region. Specifically, our coordinate transformation method transforms the original parallelogram geometry to a rectangle geometry, based on which, we determine the decision regions of the new constellations. Then, we adopt the wedge probability computation method to facilitate the derivation of the SPER based on the new decision regions. There are totally three basic wedge prototypes, discussed in Appendix A. Corresponding to these three wedge prototypes, we derive the corresponding three wedge probabilities in Appendix A, i.e., P_{w_i} for $i \in \{1,2,3\}$, based on which, we will later derive the SPER of the system.

The following lemma derives the coordinate transformation matrix at the relay.

Lemma 1: The coordinate transformation matrix $\mathbf{C}$, which transforms the exact parallelogram-shaped IRC to a rectangle centered at origin point, and preserve the length of each side in exact IRC is given by

$$\mathbf{C} = \mathbf{Q}\mathbf{A}^{-1}, \tag{9}$$

where $\mathbf{Q}$ is the eigenvector matrix for $\mathbf{B} = \mathbf{A}^T\Sigma^{-1}\mathbf{A}$ given in (47), shown as

$$\mathbf{Q} = \begin{bmatrix} \frac{\mathbf{B}(1,2)}{(\lambda_1-\lambda_2)\sqrt{\frac{\mathbf{B}(1,1)-\lambda_1}{\lambda_2-\lambda_1}}} & \sqrt{\frac{\mathbf{B}(1,1)-\lambda_1}{\lambda_2-\lambda_1}} \\ \sqrt{\frac{\mathbf{B}(1,1)-\lambda_1}{\lambda_2-\lambda_1}} & -\frac{\mathbf{B}(1,2)}{(\lambda_1-\lambda_2)\sqrt{\frac{\mathbf{B}(1,1)-\lambda_1}{\lambda_2-\lambda_1}}} \end{bmatrix}, \tag{10}$$

$$\mathbf{A}^{-1} = \begin{bmatrix} \frac{\Re\{h_{1\mathcal{R}}\}}{2|h_{1\mathcal{R}}|} & \frac{\Re\{h_{2\mathcal{R}}\}}{2|h_{2\mathcal{R}}|} \\ \frac{\Im\{h_{1\mathcal{R}}\}}{2|h_{1\mathcal{R}}|} & \frac{\Im\{h_{2\mathcal{R}}\}}{2|h_{2\mathcal{R}}|} \end{bmatrix}.$$

where the eigenvalues λ_1 and λ_2 are derived in (48).

Proof: Please refer to Appendix B. ■

Now, we will determine the decision regions of the new IRC. Denote by $\overline{\mathbf{V}}_i$ the constellation point and $\bar{Z}$ the received signal point $(\Re\{y_{\mathcal{R}}\}, \Im\{y_{\mathcal{R}}\})$ after the coordinate transformation by matrix $\mathbf{C}$, respectively. Let us denote $\bar{\Omega}_{\overline{\mathbf{V}}_i}$ the decision region corresponding to $\overline{\mathbf{V}}_i$, and define the boundary based on the Voronoi rule

$$\begin{aligned} &\bar{\Omega}_{\overline{\mathbf{V}}_1}: \left\{\Re\{\bar{Z}\} - \Im\{\bar{Z}\} > 0\right\} \text{and} \left\{\Re\{\bar{Z}\} + \Im\{\bar{Z}\} \le 0\right\}, \\ &\bar{\Omega}_{\overline{\mathbf{V}}_2}: \left\{\Re\{\bar{Z}\} - \Im\{\bar{Z}\} > 0\right\} \text{and} \left\{\Re\{\bar{Z}\} + \Im\{\bar{Z}\} > 0\right\}, \\ &\bar{\Omega}_{\overline{\mathbf{V}}_3}: \left\{\Re\{\bar{Z}\} - \Im\{\bar{Z}\} \le 0\right\} \text{and} \left\{\Re\{\bar{Z}\} + \Im\{\bar{Z}\} > 0\right\}, \\ &\bar{\Omega}_{\overline{\mathbf{V}}_4}: \left\{\Re\{\bar{Z}\} - \Im\{\bar{Z}\} \le 0\right\} \text{and} \left\{\Re\{\bar{Z}\} + \Im\{\bar{Z}\} \le 0\right\}. \end{aligned} \tag{11}$$

From (11), we can see that the decision regions form a rectangle geometry with simple decision boundary lines[3]. In Fig. 2, we present the constellation at relay after the coordinate transformation and its decision regions.

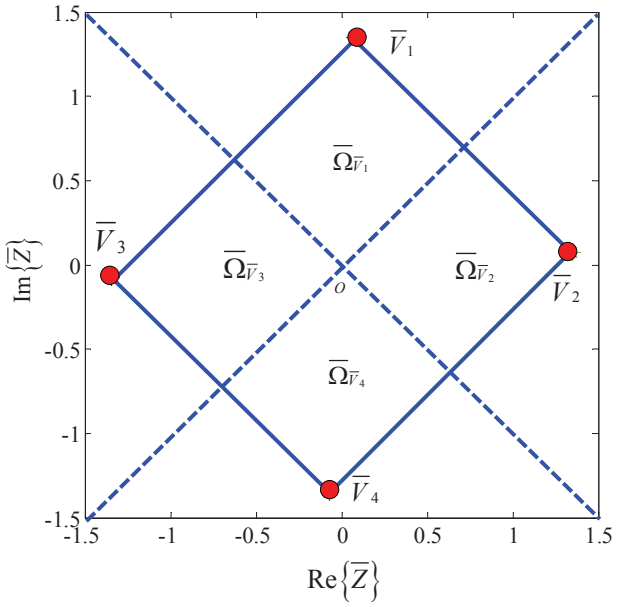

Fig. 2. Received constellation at relay after coordinate transformation.

With the setup of the coordinate transformed IRC and its corresponding decision regions, we use the wedge probability computation method to facilitate the derivation of the SPER in (8). Firstly, we focus on the probabilities $P(\sqrt{E_{\mathcal{R}}}x_{\mathcal{R}} = k|T_i)$, $k \in \{\pm\kappa_1, \pm\kappa_2\}$, at the relay. We calculate the probabilities that the relay detects the received signal successfully, i.e., $P(\sqrt{E_{\mathcal{R}}}x_{\mathcal{R}} = \kappa_1|T_1)$ and $P(\sqrt{E_{\mathcal{R}}}x_{\mathcal{R}} = \kappa_2|T_2)$, by P_{w_3} defined in equations (42), and calculate the probabilities that the relay makes wrong decisions, i.e., $P(\sqrt{E_{\mathcal{R}}}x_{\mathcal{R}} \in \{\pm\kappa_2, -\kappa_1\}|T_1)$ and $P(\sqrt{E_{\mathcal{R}}}x_{\mathcal{R}} \in \{\pm\kappa_1, -\kappa_2\}|T_2)$, by P_{w_1} defined in equations (40).

In particular, the probability that the relay detects the received signal $y_{\mathcal{R}}$ successfully, given T_1 is sent, is

$$\begin{aligned} &P(\sqrt{E_{\mathcal{R}}}x_{\mathcal{R}} = \kappa_1|T_1) \\ &= \int_0^{\infty} d(\Im\{\bar{Z}\}) \int_{-\Im\{\bar{Z}\}}^{\Im\{\bar{Z}\}} f_{\overline{Z}}\left(\bar{Z}; \Re\left\{\overline{\mathbf{V}}_1\right\}, \Im\left\{\overline{\mathbf{V}}_1\right\}\right) d(\Re\{\bar{Z}\}) \\ &= P_{w_3}\left(||\bar{V}_1||/\sigma^2, |\arg(\bar{V}_1) - \theta|, |\frac{\pi}{2} - \arg(\bar{V}_1) + \theta|\right), \end{aligned} \tag{12}$$

where $f_{\overline{Z}}(\cdot)$ is the probability density function of $\overline{Z}$ given in (44), $\overline{\mathbf{V}}_i(1)$ and $\overline{\mathbf{V}}_i(2)$ represent the horizontal coordinate and vertical coordinate of $\overline{\mathbf{V}}_i$, respectively, $||\bar{V}_i||$ and $\arg(\bar{V}_i)$ denote the magnitude and argument of a vector $O\bar{V}_i$ with O the origin, respectively, and $\theta = \arcsin\left(\sqrt{\frac{\mathbf{B}(1,1)-\lambda_1}{\lambda_2-\lambda_1}}\right)$ is the rotation angle defined in the last paragraph of Appendix B,

Similar to (12), we can obtain $P(\sqrt{E_{\mathcal{R}}}x_{\mathcal{R}} = k|T_1)$ for $k \in \{\pm\kappa_2, -\kappa_1\}$ and the probabilities that relay detects the received signal $y_{\mathcal{R}}$ both successfully and unsuccessfully, given T_2 is sent, as shown in (13). According to the law of total probability, $P(\sqrt{E_{\mathcal{R}}}x_{\mathcal{R}} = -\kappa_1|T_1) = 1 - \sum_{k\in\{\kappa_1,\pm\kappa_2\}} P(\sqrt{E_{\mathcal{R}}}x_{\mathcal{R}} = k|T_1)$ and $P(\sqrt{E_{\mathcal{R}}}x_{\mathcal{R}} = -\kappa_1|T_2) = 1 - \sum_{k\in\{\kappa_1,\pm\kappa_2\}} P(\sqrt{E_{\mathcal{R}}}x_{\mathcal{R}} = k|T_2)$.

Then we consider the conditional error probabilities,

[3]Note that the real decision boundary lines are slightly different from the perpendicular bisectors of Voronoi diagram after coordinate transformation. And this is the reason that the SPER results of coordinate transformation have notably little difference in low SNR comparing with its counterpart of exact constellation. As the SNR goes larger, the real decision boundary lines are coincide with the perpendicular bisectors.

$$
\begin{aligned}
P(\sqrt{E_{\mathcal{R}}}x_{\mathcal{R}} = \kappa_2|T_1) &= P_{w_1}\left(||\bar{V}_1||/\sigma^2, |\frac{\pi}{2} - \arg(\bar{V}_1) + \theta|, |\pi - \arg(\bar{V}_1) + \theta|\right),\\
P(\sqrt{E_{\mathcal{R}}}x_{\mathcal{R}} = -\kappa_2|T_1) &= P_{w_1}\left(||\bar{V}_1||/\sigma^2, |\arg(\bar{V}_1) - \theta|, |\arg(\bar{V}_1) - \theta| + \frac{\pi}{2}\right),\\
P(\sqrt{E_{\mathcal{R}}}x_{\mathcal{R}} = \kappa_2|T_2) &= P_{w_3}\left(||\bar{V}_2||/\sigma^2, |\theta - \arg(\bar{V}_2)|, \frac{\pi}{2} - |\theta - \arg(\bar{V}_2)|\right),\\
P(\sqrt{E_{\mathcal{R}}}x_{\mathcal{R}} = \kappa_1|T_2) &= P_{w_1}\left(||\bar{V}_2||/\sigma^2, \frac{\pi}{2} - |\theta - \arg(\bar{V}_2)|, \pi - |\theta - \arg(\bar{V}_2)|\right),\\
P(\sqrt{E_{\mathcal{R}}}x_{\mathcal{R}} = -\kappa_1|T_2) &= P_{w_1}\left(||\bar{V}_2||/\sigma^2, |\theta - \arg(\bar{V}_2)|, |\theta - \arg(\bar{V}_2)| + \frac{\pi}{2}\right).
\end{aligned}
\tag{13}
$$

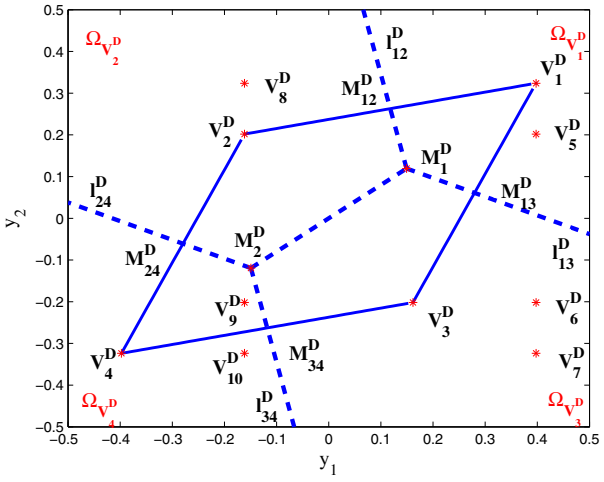

Fig. 3. Instantaneous destination constellation for network coded power adaptation scheme, where dashed lines represent boundaries of decision regions $\Omega_i^{\mathcal{D}}$.

$P(\mathcal{E}|k, T_i)$, at the destination. We establish an *instantaneous destination constellation* (IDC) with X-axis being y_1 and Y-axis being y_2 based on the minimum Euclidean distance detection, as shown in Fig. 3. When the relay detects the received signal successfully, we define four reference points as

$$
\begin{aligned}
V_1^{\mathcal{D}} &= (\sqrt{E_1}|h_{1\mathcal{D}}| + \sqrt{E_2}|h_{2\mathcal{D}}|, \kappa_1|h_{\mathcal{R}\mathcal{D}}|),\\
V_2^{\mathcal{D}} &= (-\sqrt{E_1}|h_{1\mathcal{D}}| + \sqrt{E_2}|h_{2\mathcal{D}}|, \kappa_2|h_{\mathcal{R}\mathcal{D}}|),\\
V_3^{\mathcal{D}} &= (\sqrt{E_1}|h_{1\mathcal{D}}| - \sqrt{E_2}|h_{2\mathcal{D}}|, -\kappa_2|h_{\mathcal{R}\mathcal{D}}|),\\
V_4^{\mathcal{D}} &= (-\sqrt{E_1}|h_{1\mathcal{D}}| - \sqrt{E_2}|h_{2\mathcal{D}}|, -\kappa_1|h_{\mathcal{R}\mathcal{D}}|).
\end{aligned}
\tag{14}
$$

Similar to the IRC and our previous work [27], the decision regions of the IDC are segmented by the perpendicular bisectors of each edge in the parallelogram according to the Voronoi rule [26]. In our previous work [27], we did not assume carrier phase synchronization of sources-destination channel and relay-destination channel. Instead, at destination, we take the l_1 norm of signals y_1 and y_2 as X-axis and Y-axis, respectively. In this work, specifically, rays $l_{12}^{\mathcal{D}}$, $l_{13}^{\mathcal{D}}$, $l_{24}^{\mathcal{D}}$ and $l_{34}^{\mathcal{D}}$ are perpendicular bisectors of sides $V_1^{\mathcal{D}}V_2^{\mathcal{D}}$, $V_1^{\mathcal{D}}V_3^{\mathcal{D}}$, $V_2^{\mathcal{D}}V_4^{\mathcal{D}}$ and $V_3^{\mathcal{D}}V_4^{\mathcal{D}}$, respectively. $M_1^{\mathcal{D}}$ is the crossing point of ray $l_{12}^{\mathcal{D}}$ and $l_{13}^{\mathcal{D}}$, and $M_2^{\mathcal{D}}$ is the crossing point of ray $l_{24}^{\mathcal{D}}$ and $l_{34}^{\mathcal{D}}$. Line segment $\overline{M_1^{\mathcal{D}}M_2^{\mathcal{D}}}$ is the perpendicular bisector of diagonal $\overline{V_2^{\mathcal{D}}V_3^{\mathcal{D}}}$. Then the correct decision region $V_1^{\mathcal{D}}$ at destination is

$$
\Omega_{V_1^{\mathcal{D}}} \triangleq \left\{ \frac{2\sqrt{E_1}|h_{1\mathcal{D}}|}{(\kappa_1 - \kappa_2)|h_{\mathcal{R}\mathcal{D}}|}y_1 + y_2 + M_1^{\mathcal{D}} > 0 \right\} \bigcap \left\{ \frac{2\sqrt{E_2}|h_{2\mathcal{D}}|}{(\kappa_1 + \kappa_2)|h_{\mathcal{R}\mathcal{D}}|}y_1 + y_2 + M_2^{\mathcal{D}} > 0 \right\},
\tag{15}
$$

where $M_1^{\mathcal{D}} = -\frac{1}{2}(\kappa_1+\kappa_2)|h_{\mathcal{R}\mathcal{D}}| - 2\sqrt{E_1E_2}|h_{1\mathcal{D}}||h_{2\mathcal{D}}|(\kappa_1 - \kappa_2)|h_{\mathcal{R}\mathcal{D}}|$ and $M_2^{\mathcal{D}} = -\frac{1}{2}(\kappa_1 - \kappa_2)|h_{\mathcal{R}\mathcal{D}}| - 2\sqrt{E_1E_2}|h_{1\mathcal{D}}||h_{2\mathcal{D}}|(\kappa_1 + \kappa_2)|h_{\mathcal{R}\mathcal{D}}|$. Likewise, we can obtain $\Omega_{V_i^{\mathcal{D}}}$ for $i = 2, 3, 4$.

Similar to the error probability analysis at the relay, we will show the results of the coordinate transformation and the error probability based on the new constellation at the destination. In the following lemma, we present the coordinate transformation matrix $\mathbf{C}_{\mathcal{D}}$ at the destination.

Lemma 2: At the destination, the coordinate transformation matrix $\mathbf{C}_{\mathcal{D}}$, which transform the exact IDC to a rectangle centered at the origin point, and preserve the length of each side in an exact parallelogram-shaped IDC is given by

$$
\mathbf{C}_{\mathcal{D}} = \mathbf{Q}_{\mathcal{D}}\mathbf{A}_{\mathcal{D}}^{-1},
\tag{16}
$$

where $\mathbf{Q}_{\mathcal{D}}$ is the eigenvector matrix for $\mathbf{B}_{\mathcal{D}}$ shown in (17), where $\beta_{\mathcal{D}} = |h_{\mathcal{R}\mathcal{D}}|\left(|h_{1\mathcal{D}}|(\kappa_1 + \kappa_2) + |h_{2\mathcal{D}}|(\kappa_2 - \kappa_1)\right)$, $d_1 = \sqrt{4|h_{1\mathcal{D}}|^2 + (\kappa_1 - \kappa_2)^2|h_{\mathcal{R}\mathcal{D}}|^2}$ and $d_2 = \sqrt{4|h_{2\mathcal{D}}|^2 + (\kappa_1 + \kappa_2)^2|h_{\mathcal{R}\mathcal{D}}|^2}$. Then,

$$
\mathbf{Q}_{\mathcal{D}} = \begin{bmatrix} \frac{\mathbf{B}_{\mathcal{D}}(1,2)}{(\lambda_1^{\mathcal{D}} - \lambda_2^{\mathcal{D}})\sqrt{\frac{\mathbf{B}_{\mathcal{D}}(1,1) - \lambda_1^{\mathcal{D}}}{\lambda_2^{\mathcal{D}} - \lambda_1^{\mathcal{D}}}}} & \sqrt{\frac{\mathbf{B}_{\mathcal{D}}(1,1) - \lambda_1^{\mathcal{D}}}{\lambda_2^{\mathcal{D}} - \lambda_1^{\mathcal{D}}}} \\ \sqrt{\frac{\mathbf{B}_{\mathcal{D}}(1,1) - \lambda_1^{\mathcal{D}}}{\lambda_2^{\mathcal{D}} - \lambda_1^{\mathcal{D}}}} & -\frac{\mathbf{B}_{\mathcal{D}}(1,2)}{(\lambda_1^{\mathcal{D}} - \lambda_2^{\mathcal{D}})\sqrt{\frac{\mathbf{B}_{\mathcal{D}}(1,1) - \lambda_1^{\mathcal{D}}}{\lambda_2^{\mathcal{D}} - \lambda_1^{\mathcal{D}}}}} \end{bmatrix},
\tag{18}
$$

where $\lambda_1^{\mathcal{D}}$ and $\lambda_2^{\mathcal{D}}$ are eigenvalues of $\mathbf{B}_{\mathcal{D}}$. Also, we have

$$
\mathbf{A}_{\mathcal{D}}^{-1} = \frac{1}{\beta_{\mathcal{D}}}\begin{bmatrix} (\kappa_2 - \kappa_1)d_2|h_{\mathcal{R}\mathcal{D}}| & 2d_2|h_{1\mathcal{D}}| \\ (\kappa_1 + \kappa_2)d_1|h_{\mathcal{R}\mathcal{D}}| & -2d_1|h_{2\mathcal{D}}| \end{bmatrix}.
\tag{19}
$$

Proof: Following the similar procedure of *Lemma 1*, we can obtain the coordination transformation matrix $\mathbf{C}_{\mathcal{D}}$ at destination. We complete the proof. ■

Now, we will determine the decision regions with the new coordinate transformed IDC. Denote $\overline{\mathbf{V}}_i^{\mathcal{D}}$ the constellation point and $\bar{Z}_{\mathcal{D}}$ the received signal after coordinate transformation by matrix $\mathbf{C}_{\mathcal{D}}$. Let us denote by $\bar{\Omega}_{\overline{\mathbf{V}}_i^{\mathcal{D}}}^{\mathcal{D}}$ the decision region corresponding to $\overline{\mathbf{V}}_i^{\mathcal{D}}$, where the boundary is defined

$$\mathbf{B}_{\mathcal{D}} = \frac{2}{\beta_{\mathcal{D}}^2\sigma^2}\begin{bmatrix} d_1^2(\kappa_1+\kappa_2)^2|h_{\mathcal{RD}}|^2 + 4d_1^2|h_{2\mathcal{D}}|^2 & d_1d_2(\kappa_2^2-\kappa_1^2)|h_{\mathcal{RD}}|^2 - 4d_1d_2|h_{1\mathcal{D}}||h_{2\mathcal{D}}| \\ d_1d_2(\kappa_2^2-\kappa_1^2)|h_{\mathcal{RD}}|^2 - 4d_1d_2|h_{1\mathcal{D}}||h_{2\mathcal{D}}| & d_2^2(\kappa_2-\kappa_1)^2|h_{\mathcal{RD}}|^2 + 4d_2^2|h_{2\mathcal{D}}|^2 \end{bmatrix}, \quad (17)$$

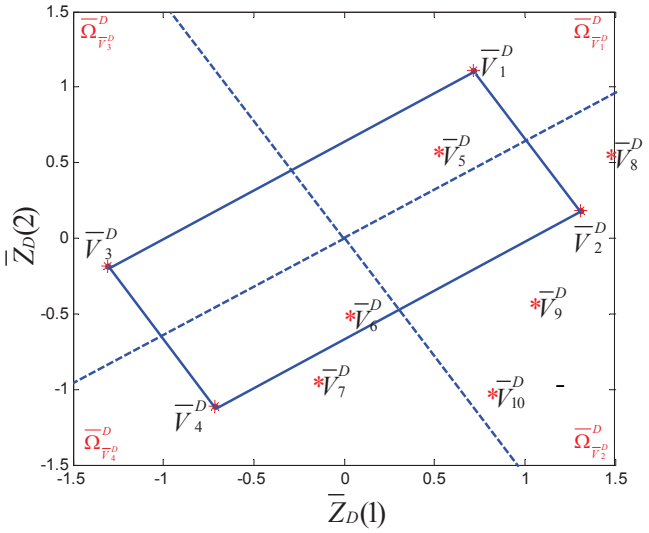

Fig. 4. Received constellation at destination after coordinate transformation.

based on the Voronoi rule

$$\begin{aligned}
\bar{\Omega}_{\bar{\mathbf{V}}_1^{\mathcal{D}}}^{\mathcal{D}} &: \left\{\bar{Z}_{\mathcal{D}}(1) - \bar{Z}_{\mathcal{D}}(2) > 0\right\} \bigcap \left\{\bar{Z}_{\mathcal{D}}(1) + \bar{Z}_{\mathcal{D}}(2) \le 0\right\}, \\
\bar{\Omega}_{\bar{\mathbf{V}}_2^{\mathcal{D}}}^{\mathcal{D}} &: \left\{\bar{Z}_{\mathcal{D}}(1) - \bar{Z}_{\mathcal{D}}(2) > 0\right\} \bigcap \left\{\bar{Z}_{\mathcal{D}}(1) + \bar{Z}_{\mathcal{D}}(2) > 0\right\}, \\
\bar{\Omega}_{\bar{\mathbf{V}}_3^{\mathcal{D}}}^{\mathcal{D}} &: \left\{\bar{Z}_{\mathcal{D}}(1) - \bar{Z}_{\mathcal{D}}(2) \le 0\right\} \bigcap \left\{\bar{Z}_{\mathcal{D}}(1) + \bar{Z}_{\mathcal{D}}(2) > 0\right\}, \\
\bar{\Omega}_{\bar{\mathbf{V}}_4^{\mathcal{D}}}^{\mathcal{D}} &: \left\{\bar{Z}_{\mathcal{D}}(1) - \bar{Z}_{\mathcal{D}}(2) \le 0\right\} \bigcap \left\{\bar{Z}_{\mathcal{D}}(1) + \bar{Z}_{\mathcal{D}}(2) \le 0\right\},
\end{aligned} \quad (20)$$

$\bar{Z}_{\mathcal{D}}(1)$ and $\bar{Z}_{\mathcal{D}}(2)$ represent the horizontal coordinate and vertical coordinate of $\bar{Z}_{\mathcal{D}}$, respectively. In Fig. 4, we present the constellation at destination after the coordinate transformation and its decision regions.

When T_1 and T_2 are transmitted by the sources, the error probabilities at the destination, given that the relay transmits the correct symbol, is denoted by $P\left(\mathcal{E}|\sqrt{E_{\mathcal{R}}}x_{\mathcal{R}} = \kappa_1, T_1\right)$ and $P\left(\mathcal{E}|\sqrt{E_{\mathcal{R}}}x_{\mathcal{R}} = \kappa_2, T_2\right)$, respectively. Based on the decision regions of the new IDC, regarding the probability $P\left(\mathcal{E}|\sqrt{E_{\mathcal{R}}}x_{\mathcal{R}} = \kappa_1, T_1\right)$, we have

$$\begin{aligned}
&P\left(\mathcal{E}|\sqrt{E_{\mathcal{R}}}x_{\mathcal{R}} = \kappa_1, T_1\right) \\
&= \int_0^{\infty} d(\bar{Z}_{\mathcal{D}}(2)) \int_{-\bar{Z}_{\mathcal{D}}(2)}^{\bar{Z}_{\mathcal{D}}(2)} f_{\overline{Z}_{\mathcal{D}}}\left(\bar{Z}_{\mathcal{D}}; \overline{\mathbf{V}}_i^{\mathcal{D}}(1), \overline{\mathbf{V}}_i^{\mathcal{D}}(2)\right) d(\bar{Z}_{\mathcal{D}}(1)), \\
&= P_{w_3}\left(||\bar{V}_1^{\mathcal{D}}||/\sigma^2, |\arg(\bar{V}_1^{\mathcal{D}}) - \theta_{\mathcal{D}}|, |\frac{\pi}{2} - \arg(\bar{V}_1^{\mathcal{D}}) + \theta_{\mathcal{D}}|\right)
\end{aligned} \quad (21)$$

where $f_{\overline{Z}_{\mathcal{D}}}(\cdot)$ is the probability density function of $\bar{Z}_{\mathcal{D}}$, $\overline{\mathbf{V}}_i^{\mathcal{D}}(1)$ and $\overline{\mathbf{V}}_i^{\mathcal{D}}(2)$ represent the horizontal coordinate and vertical coordinate of $\overline{\mathbf{V}}_i^{\mathcal{D}}$, respectively, $\theta_{\mathcal{D}} = \arcsin\left(\sqrt{\frac{\mathbf{B}_{\mathcal{D}}(1,1)-\lambda_1^{\mathcal{D}}}{\lambda_2^{\mathcal{D}}-\lambda_1^{\mathcal{D}}}}\right)$ is the rotation angle corresponding to rotation matrix $\mathbf{Q}_{\mathcal{D}}$. Similar to (21), regarding the probability $P\left(\mathcal{E}|\sqrt{E_{\mathcal{R}}}x_{\mathcal{R}} = \kappa_2, T_2\right)$, we have

$$\begin{aligned}
&P\left(\mathcal{E}|\sqrt{E_{\mathcal{R}}}x_{\mathcal{R}} = \kappa_2, T_2\right) \\
&= P_{w_3}\left(||\bar{V}_2^{\mathcal{D}}||/\sigma^2, \frac{1}{2}|\theta_{\mathcal{D}} - \arg(\bar{V}_2^{\mathcal{D}})|, \frac{\pi}{2} - |\theta_{\mathcal{D}} - \arg(\bar{V}_2^{\mathcal{D}})|\right).
\end{aligned} \quad (22)$$

When the relay detects the received signal unsuccessfully, the reference points in (14) will change according to the incorrect relay decisions. In particular, if sources transmit T_1 and the relay wrongly forwards $\kappa_2, -\kappa_2, -\kappa_1$, then the reference point $V_1^{\mathcal{D}}$ in Fig. 3 will change to $V_5^{\mathcal{D}}$, $V_6^{\mathcal{D}}$, and $V_7^{\mathcal{D}}$, respectively. And if sources transmit T_2 and the relay wrongly forwards $\kappa_1, -\kappa_2, -\kappa_1$, then the reference point $V_2^{\mathcal{D}}$ in Fig. 3 will change to $V_8^{\mathcal{D}}$, $V_9^{\mathcal{D}}$, and $V_{10}^{\mathcal{D}}$, respectively. Denote $\bar{V}_i^{\mathcal{D}}$ for $i \in \{5, \cdots, 10\}$ the reference point after coordinate transformation.

In the case when T_1 is transmitted by the sources, and the relay wrongly forwards $\kappa_2, -\kappa_2, -\kappa_1$, the error probabilities that destination makes wrong decisions are given by (23), when $k_1 = \kappa_2, -\kappa_2, -\kappa_1$, then $j = 5, 6, 7$, respectively.

In the case when T_2 is transmitted by the sources, and the relay wrongly forwards $\kappa_1, -\kappa_2, -\kappa_1$, the error probabilities that destination makes wrong decisions are given by (24), where when $k_1 = \kappa_1, -\kappa_2, -\kappa_1$, then $l = 8, 9, 10$, respectively.

V. System Optimization

In this section, we obtain the optimal power levels by separately discussing the derivations of the power scaling factor and the power adaptation factors, respectively. We first develop a practical method at the relay side to address the error propagation problem. With the designed methods, the system is proved to achieve a full diversity when the relay cannot detect all the received signals successfully. Specifically, we propose a power scaling scheme where the relay power adapts to the channel conditions. In order to obtain the power scaling factor, we model a complex MARC system as a degraded virtual one-source one-relay one destination model (triangle model), and show that the relay power should be chosen to balance the SNRs of source-relay channel and relay-destination channel. Moreover, we formulate a sub-optimal Euclidean distance optimization problem to obtain the optimized power adaptation parameters $\tilde{\kappa}_1$ and $\tilde{\kappa}_2$ that minimize the end-to-end SPER.

A. The Design of Power Scaling Factor at the Relay

Before introducing the design of power scaling factor at the relay, we present the diversity performance of the proposed PANC and the CXNC scheme in the following Theorem 1. In the CXNC scheme, we do not consider any relay processes to identify or drop erroneous symbols and thus mitigate error propagation from source-relay channel to destination, e.g., outage event detection, CRC, and etc. In order to measure

$$P\left(\mathcal{E}|\sqrt{E_{\mathcal{R}}}x_{\mathcal{R}}=k_1,T_1\right)=\begin{cases}1-P_{w_3}\left(||\bar{V}_j^{\mathcal{D}}||/\sigma^2,|\arg(\bar{V}_j^{\mathcal{D}})-\theta_{\mathcal{D}}|,|\frac{\pi}{2}-\arg(\bar{V}_j^{\mathcal{D}})+\theta_{\mathcal{D}}|\right), & \text{when } V_j^{\mathcal{D}}\in\Omega_{V_1^{\mathcal{D}}},\\ 1-P_{w_1}\left(||\bar{V}_j^{\mathcal{D}}||/\sigma^2,|\frac{\pi}{2}-\theta_{\mathcal{D}}+\arg(\bar{V}_j^{\mathcal{D}})|,|\pi-\theta_{\mathcal{D}}+\arg(\bar{V}_j^{\mathcal{D}})|\right), & \text{when } V_j^{\mathcal{D}}\notin\Omega_{V_1^{\mathcal{D}}},\end{cases} \tag{23}$$

$$P\left(\mathcal{E}|\sqrt{E_{\mathcal{R}}}x_{\mathcal{R}}=k_2,T_2\right)=\begin{cases}1-P_{w_3}\left(||\bar{V}_l^{\mathcal{D}}||/\sigma^2,|\arg(\bar{V}_l^{\mathcal{D}})+\theta_{\mathcal{D}}|,|\frac{\pi}{2}-\arg(\bar{V}_l^{\mathcal{D}})-\theta_{\mathcal{D}}|\right), & \text{when } V_l^{\mathcal{D}}\in\Omega_{V_2^{\mathcal{D}}},\\ 1-P_{w_1}\left(||\bar{V}_l^{\mathcal{D}}||/\sigma^2,|\pi-\arg(\bar{V}_l^{\mathcal{D}})-\theta_{\mathcal{D}}|,|\frac{3\pi}{2}-\arg(\bar{V}_l^{\mathcal{D}})-\theta_{\mathcal{D}}|\right), & \text{when } V_l^{\mathcal{D}}\notin\Omega_{V_2^{\mathcal{D}}},\end{cases} \tag{24}$$

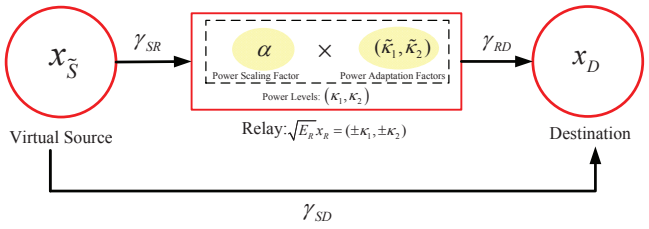

Fig. 5. Virtual channel model. In particular, the channel gains $\gamma_{\mathcal{SR}}$ and $\gamma_{\mathcal{SD}}$ with respect to virtual channels will be introduced in detail in the following paragraph. $x_{\tilde{S}}$ is the virtual source message, which is generated from the original transmitted signal as $x_{\tilde{S}}=x_1\boxplus x_2$. $x_{\mathcal{R}}$ is the real transmitted signal from the relay to destination. And $x_{\mathcal{D}}$ is also equal to $x_1\boxplus x_2$.

the performance of PANC and CXNC schemes in the high SNR regime, the diversity order D [28] is calculated by

$$D=-\lim_{\rho\to\infty}\frac{\log P\left((\hat{x}_1,\hat{x}_2)\neq(x_1,x_2)\right)}{\log\rho}, \tag{25}$$

where ρ represents the transmission SNR, (x_1,x_2) is the source symbol pair, $(\hat{x}_1,\hat{x}_2)$ is the decoded symbol pair at destination and $P\left((\hat{x}_1,\hat{x}_2)\neq(x_1,x_2)\right)$ is the SPER.

Theorem 1: Without power scaling factor at the relay, both the PANC scheme and the CXNC scheme can only achieve the diversity of one in MARC system for error propagation issue.

Proof: Please refer to Appendix C. ■

From *Theorem 1*, we can see that the error propagation from the source-relay hop degrades the performance of the system. In this case, we adopt a power scaling factor at the relay to mitigate the effect of error propagation by adjusting the relay transmission power to the channel conditions. Such a link adaptive ratio (LAR) was first introduced for the single-source decode-and-forward (DF) system in [29]. However, LAR cannot be directly applied to the multi-user PANC system.

To extend the LAR concept, we first develop a virtual channel model for the source-relay-destination link, as shown in Fig. 4. In the first phase, the two sources transmit to the relay simultaneously. For such multiple-access channel, the union bound of SPER in a multiple-access channel (MAC) is

$$\begin{aligned}P_{\text{MAC}}\leq P_{\text{MAC}}^{\text{upper}}&=Q_1\left(\sqrt{2E_1|h_{1\mathcal{R}}|^2/\sigma^2}\right)\\&+Q_1\left(\sqrt{2E_2|h_{2\mathcal{R}}|^2/\sigma^2}\right)\\&+Q_1\left(\sqrt{2|\sqrt{E_1}h_{1\mathcal{R}}+\sqrt{E_2}h_{2\mathcal{R}}|^2/\sigma^2}\right),\end{aligned} \tag{26}$$

where the first term in the right side of (26) represents the error probability that the relay fails to decode x_1 and successfully decode x_2. Likewise, the second term is the error probability that the relay fails to decode x_2 while successfully decode x_1. Also, the third term is the error probability that the relay fails to decode both x_1 and x_2. The union bound $P_{\text{MAC}}^{\text{upper}}$ can be further approximated as (27), which is quite tight when $E_1|h_{1\mathcal{R}}|^2/\sigma^2$, $E_2|h_{2\mathcal{R}}|^2/\sigma^2$, $|\sqrt{E_1}h_{1\mathcal{R}}+\sqrt{E_2}h_{2\mathcal{R}}|^2/\sigma^2$ and their difference are reasonably large, as the one-dimensional Q-function $Q_1(x)$ decays fast as x grows. The advantage of such an approximation is that we can now model the multiple access source-relay channel as a single-input single-output channel with the input being the virtual source message $x_{\tilde{S}}=x_1\boxplus x_2$ and the instantaneous received SNR being $\gamma_{\mathcal{SR}}\triangleq\min(E_1|h_{1\mathcal{R}}|^2/\sigma^2,E_2|h_{2\mathcal{R}}|^2/\sigma^2,|\sqrt{E_1}h_{1\mathcal{R}}+\sqrt{E_2}h_{2\mathcal{R}}|^2)/\sigma^2$, which represents the SNR of the worse source-relay channel[4]. The idea of regarding a virtual source message as network coded sources' signals is that we implement network coding at the relay. Thus, the virtual transmitting information from source to destination via the aid of relay becomes the same, i.e., $x_{\tilde{S}}=x_{\mathcal{R}}$. Following the similar derivation of $\gamma_{\mathcal{SR}}$, we can model the multiple access source-destination channel as a point-to-point channel with the instantaneous received SNR, denoted by $\gamma_{\mathcal{SD}}$, which is defined

$$\gamma_{\mathcal{SD}}\triangleq\min\left(\frac{E_1|h_{1\mathcal{D}}|^2}{\sigma^2},\frac{E_2|h_{2\mathcal{D}}|^2}{\sigma^2},\frac{|\sqrt{E_1}|h_{1\mathcal{D}}|+\sqrt{E_2}|h_{2\mathcal{D}}||^2}{\sigma^2}\right). \tag{28}$$

So far, we have successfully reduced the complex MARC system to a traditional triangle model. Based on the conclusion in [29], the power scaling factor α with instantaneous $\gamma_{\mathcal{SR}}$ and $\gamma_{\mathcal{RD}}$ is

$$\alpha=\min\left(\frac{\gamma_{\mathcal{SR}}}{\gamma_{\mathcal{RD}}},1\right). \tag{29}$$

Note that, the instantaneous received SNR $\gamma_{\mathcal{RD}}$ can be replaced by statistical received SNR $\bar{\gamma}_{\mathcal{RD}}$, which will be proved in Appendix D. The advantage of using $\bar{\gamma}_{\mathcal{RD}}$ to obtain α is that the relay does not need the feedback of relay-destination channel. Later, we will show that using both instantaneous and statistical relay-destination received SNR can result in a full diversity in the proposed PANC scheme.

Theorem 2: Given the instantaneous source-relay received SNR, and instantaneous (or statistical) relay-destination re-

[4]Note that our approximation is different from the equivalent channels shown in [14] [30], in which the authors consider an orthogonal MARC system.

$$P_{\text{MAC}}^{U} \approx Q_1\left(\sqrt{2\min\left[E_1|h_{1\mathcal{R}}|^2/\sigma^2, E_2|h_{2\mathcal{R}}|^2/\sigma^2, |\sqrt{E_1}h_{1\mathcal{R}}+\sqrt{E_2}h_{2\mathcal{R}}|^2/\sigma^2\right]}\right), \tag{27}$$

ceived SNR, the power scaled PANC scheme can achieve a diversity of two, i.e., the full diversity, in the MARC system with two sources, while the power scaled conventional NC scheme can only achieve the diversity of one even with the power scaling.

Proof: Please refer to Appendix D. ■

B. The Design of Power Adaptation Factors

From the derivations of the instantaneous system SPER in Section IV, we note that the expressions of the SPER depends on the power adaptation levels $\tilde{\kappa}_1$ and $\tilde{\kappa}_2$ at the relay. To minimize the SPER requires an optimization of $\tilde{\kappa}_1$ and $\tilde{\kappa}_2$. However, directly minimizing the SPER is very complicated and leads to no closed form expressions for $\tilde{\kappa}_1$ and $\tilde{\kappa}_2$. Here, we propose a sub-optimal criterion for the instantaneous SPER minimization, i.e., maximizing the minimum Euclidean distances of the coordinate transformed IDC [31]. Since we consider slow fading channel, i.e., the channel coefficients are constant with a transmission period, the power adaptation factors $\tilde{\kappa}_1$ and $\tilde{\kappa}_2$ are optimized for each transmission period. For the coordinate transformed IDC, we only consider the two edges of the rectangle, since the two edges are always less than the diagonals of the rectangle. The Euclidean distance optimization problem under the power constraint is formulated as

$$\begin{aligned}(\tilde{\kappa}_1^*, \tilde{\kappa}_2^*) = \arg\max_{\tilde{\kappa}_1,\tilde{\kappa}_2} \min_{j=2,3} \left\{||\bar{V}_1^{\mathcal{D}} - \bar{V}_j^{\mathcal{D}}||^2\right\} \\ \text{s. t. } \tilde{\kappa}_1^2 + \tilde{\kappa}_2^2 \le 2E_{\mathcal{R}}^{\text{ave}}, \ \ \tilde{\kappa}_1, \tilde{\kappa}_2 \in \mathbb{R},\end{aligned} \tag{30}$$

where the lengths of the rectangle's two edges are $\overline{\bar{V}_1^{\mathcal{D}}\bar{V}_2^{\mathcal{D}}} = \overline{V_1^{\mathcal{D}}V_2^{\mathcal{D}}} = ||V_1^{\mathcal{D}} - V_2^{\mathcal{D}}||^2 = 4E_1|h_{1\mathcal{D}}|^2 + \alpha|h_{\mathcal{R}\mathcal{D}}|^2(\tilde{\kappa}_1 - \tilde{\kappa}_2)^2$ and $\overline{\bar{V}_1^{\mathcal{D}}\bar{V}_3^{\mathcal{D}}} = \overline{V_1^{\mathcal{D}}V_3^{\mathcal{D}}} = 4E_2|h_{2\mathcal{D}}|^2 + \alpha|h_{\mathcal{R}\mathcal{D}}|^2(\tilde{\kappa}_1 + \tilde{\kappa}_2)^2$ because the coordinate transformation of IDC preserves the length of the geometry's sides as introduced in Appendix B. Defining $\mathcal{V}$ as the set of $\left\{\overline{\bar{V}_1^{\mathcal{D}}\bar{V}_2^{\mathcal{D}}}, \overline{\bar{V}_1^{\mathcal{D}}\bar{V}_3^{\mathcal{D}}}\right\}$, and introducing a variable $u \triangleq \min\{\mathcal{V}\}$, after some manipulations, the Euclidean distance optimization problem in (30) can be further described as a maximization problem

$$\begin{aligned}&\max u \\ &\text{s. t. } -(4E_1|h_{1\mathcal{D}}|^2 + \alpha|h_{\mathcal{R}\mathcal{D}}|^2(\tilde{\kappa}_1 - \tilde{\kappa}_2)^2) \le -u, \\ &\quad -(4E_2|h_{2\mathcal{D}}|^2 + \alpha|h_{\mathcal{R}\mathcal{D}}|^2(\tilde{\kappa}_1 + \tilde{\kappa}_2)^2) \le -u, \\ &\quad \tilde{\kappa}_1^2 + \tilde{\kappa}_2^2 \le 2E_{\mathcal{R}}^{\text{ave}}.\end{aligned} \tag{31}$$

Since the objective function of the new maximization problem is an affine function and the constraints are quadratic functions of $\tilde{\kappa}_1$ and $\tilde{\kappa}_2$ in (31), it is a convex optimization problem. We can adopt the Lagrange Multiplier method to obtain the solutions. The Lagrange equation is given by

$$\begin{aligned}&L(\tilde{\kappa}_1, \tilde{\kappa}_2, u, \mu_1, \mu_2, \mu_3) \\ &= u + \mu_1(u - 4E_1|h_{1\mathcal{D}}|^2 - \alpha|h_{\mathcal{R}\mathcal{D}}|^2(\tilde{\kappa}_1 - \tilde{\kappa}_2)^2) \\ &+ \mu_2(u - 4E_2|h_{2\mathcal{D}}|^2 - \alpha|h_{\mathcal{R}\mathcal{D}}|^2(\tilde{\kappa}_1 + \tilde{\kappa}_2)^2) \\ &+ \mu_3(\tilde{\kappa}_1^2 + \tilde{\kappa}_2^2 - E_{\mathcal{R}}^{\text{ave}}).\end{aligned} \tag{32}$$

Specifically, when $\mu_i = 0$, it represents that the ith constraint is not binding. Then we can ignore the ith constraint, and derive the optimal $\tilde{\kappa}_1$ and $\tilde{\kappa}_2$ combining the Lagrangian function and other KKT conditions. When $\mu_i \neq 0$, it represents that the ith constraint is binding. Then we can obtain an equality of parameters $\tilde{\kappa}_1$ and $\tilde{\kappa}_2$ with respect to the ith constraint. For instance, when $\mu_1 \neq 0$, we will have

$$u - 4E_1|h_{1\mathcal{D}}|^2 - \alpha|h_{\mathcal{R}\mathcal{D}}|^2(\tilde{\kappa}_1 - \tilde{\kappa}_2)^2 = 0. \tag{33}$$

In this case, there are totally 8 solutions with respect to the value of μ_i, among which, we present positive real $\tilde{\kappa}_1$ and $\tilde{\kappa}_2$ that correspond to the maximum u as follows.

$$\begin{aligned}\tilde{\kappa}_1^* = \frac{1}{2}\Bigg(&\sqrt{\frac{2\left(\alpha E_{\mathcal{R}}^{\text{ave}}|h_{\mathcal{R}\mathcal{D}}|^2 + E_2|h_{2\mathcal{D}}|^2 - E_1|h_{1\mathcal{D}}|^2\right)}{\alpha|h_{\mathcal{R}\mathcal{D}}|^2}} \\ &+\sqrt{\frac{2\left(\alpha E_{\mathcal{R}}^{\text{ave}}|h_{\mathcal{R}\mathcal{D}}|^2 + E_1|h_{1\mathcal{D}}|^2 - E_2|h_{2\mathcal{D}}|^2\right)}{\alpha|h_{\mathcal{R}\mathcal{D}}|^2}}\Bigg), \\ \tilde{\kappa}_2^* = \frac{1}{2}\Bigg(&\sqrt{\frac{2\left(\alpha E_{\mathcal{R}}^{\text{ave}}|h_{\mathcal{R}\mathcal{D}}|^2 + E_1|h_{1\mathcal{D}}|^2 - E_2|h_{2\mathcal{D}}|^2\right)}{\alpha|h_{\mathcal{R}\mathcal{D}}|^2}} \\ &-\sqrt{\frac{2\left(\alpha E_{\mathcal{R}}^{\text{ave}}|h_{\mathcal{R}\mathcal{D}}|^2 + E_2|h_{2\mathcal{D}}|^2 - E_1|h_{1\mathcal{D}}|^2\right)}{\alpha|h_{\mathcal{R}\mathcal{D}}|^2}}\Bigg).\end{aligned} \tag{34}$$

In summary, combining the results of power scaling factor given in (29) and optimal power adaptation factors given in (34), the optimal power level at the relay is given by $\kappa_i = \alpha\tilde{\kappa}_i^*$ for $i = 1, 2$.

VI. Discussion

A. Extension to Coded System

For the coded case, we assume that channel codes, e.g., LDPC codes, are applied at both sources, and the codewords $\mathbf{x}_1$ and $\mathbf{x}_2$ are transmitted by $\mathcal{S}_1$ and $\mathcal{S}_2$, respectively. At the relay, a multi-user iterative receiver (Please refer to [32] for the structure of a multi-user iterative receiver) is used to iteratively detect and decode the two sources' information. After decoding $\mathbf{x}_i$, the relay encodes the information of $\mathcal{S}_i$ with an LDPC code, and obtain the codeword $\mathbf{x}_{\mathcal{R}i}$. Assuming $\mathbf{x}_{\mathcal{R}1}$ and $\mathbf{x}_{\mathcal{R}2}$ have the same length, the relay implements the mapping operations on $\mathbf{x}_{\mathcal{R}1}$ and $\mathbf{x}_{\mathcal{R}2}$ symbol-by-symbol according to (5) in the paper, and obtain the network coded vector $\mathbf{x}_{\mathcal{R}}$, which consists of the mapping results. Specifically, for the k-th symbol in $\mathbf{x}_{\mathcal{R}i}$, i.e., $x_{\mathcal{R}i,k}$, we map the symbol pair $(x_{\mathcal{R}1,k}, x_{\mathcal{R}2,k})$ to $(\kappa_1, \kappa_2, -\kappa_2, -\kappa_1)$ according to the rule illustrated in the second paragraph of Section III in our paper, where $\kappa_1 = \alpha\tilde{\kappa}_1$ and $\kappa_2 = \alpha\tilde{\kappa}_2$.

At the destination, the receiver first processes the signals from the relay, denoted by $\mathbf{y}_2$. From the k-th signal of $\mathbf{y}_2$, denoted by $y_{2,k}$, the receiver obtains the probability density function (PDF) $p\left(y_{2,k}|x_{\mathcal{R},k} = \kappa\right)$ as

$$p\left(y_{2,k}|x_{\mathcal{R},k} = \kappa\right) = \frac{1}{\sqrt{2\pi\sigma^2}}\exp\left\{-\frac{(y_{2,k} - h_{\mathcal{R}\mathcal{D}}\kappa)^2}{2\sigma^2}\right\}. \tag{35}$$

$$l_{x_{\mathcal{R}1,k}} = \log \frac{p(y_{2,k}|x_{\mathcal{R},k}=\kappa_1)P(x_{\mathcal{R},k}=\kappa_1) + p(y_{2,k}|x_{\mathcal{R},k}=\kappa_2)P(x_{\mathcal{R},k}=\kappa_2)}{p(y_{2,k}|x_{\mathcal{R},k}=-\kappa_2)P(x_{\mathcal{R},k}=-\kappa_2) + p(y_{2,k}|x_{\mathcal{R},k}=-\kappa_1)P(x_{\mathcal{R},k}=-\kappa_1)}, \tag{36}$$

Based on $p\left(y_{2,k}|x_{\mathcal{R},k}=\kappa\right)$, we can thus obtain the log-likelihood ratio (LLR) for $x_{\mathcal{R}1,k}$ as (36), where the priori probabilities $P(x_{\mathcal{R},k}=\kappa_1)$, $P(x_{\mathcal{R},k}=\kappa_2)$, $P(x_{\mathcal{R},k}=-\kappa_1)$, and $P(x_{\mathcal{R},k}=-\kappa_2)$ are all equal to $\frac{1}{4}$. Similarly, we can calculate the LLR $l_{x_{\mathcal{R}2,k}}$. By using the LLR values $l_{x_{\mathcal{R}1,k}}$ and $l_{x_{\mathcal{R}2,k}}$ as the input of the LDPC codes implemented at the relay, we can obtain the LLR values for the information symbols of each source. We denote by $l_{x_{i,k}}^{(\mathcal{R})}$ the LLR value of the symbol $x_{i,k}$ based on the signals from the relay.

Next, for the signals from the direct source-to-destination channels, i.e., $\mathbf{y}_1$, the destination adopts a multi-user iterative receiver to iteratively detect and decode the two sources' information. The detector at destination obtains the LLR $l_{x_{i,k}}$ with $i \in \{1,2\}$ for the symbol $x_{i,k}$ based on the k-th signal from $\mathbf{y}_1$ as shown in [32].

Finally, the detector combines $l_{x_{i,k}}^{(\mathcal{R})}$ and $l_{x_{i,k}}$ together and carry the sum of the two LLRs to the decoder to update the LLR of $x_{i,k}$. After a fixed number of iterations between the detector and the decoder, the destination makes a hard decision based on the LLR value of $x_{i,k}$.

From the diversity gain point of view, since our scheme can achieve the full diversity gain in the uncoded system, it is easy to prove that it can also achieve the full diversity gain in the coded system.

B. Extension to Higher-order Modulation

Although we focus primarily on BPSK signals so far, our work can be extended to higher-order modulations. Specifically, for the PANC at relay, parameters κ_1 and κ_2 denote the higher and lower power levels, respectively. The relay transmitted signal is $x_{\mathcal{R}} = \hat{x}_1 \boxplus \hat{x}_2 = \text{sign}(|h_{1\mathcal{R}}|\Re\{\hat{x}_1\} + |h_{2\mathcal{R}}|\Re\{\hat{x}_2\}) + i\,\text{sign}(|h_{1\mathcal{R}}|\Im\{\hat{x}_1\} + |h_{2\mathcal{R}}|\Im\{\hat{x}_2\})$, where i is the unit imaginary number.

For error performance analysis, by defining $T_i = (m_1 + in_1, m_2 + in_2)$ for $m_1, m_2, n_1, n_2 \in \{\pm\kappa_1, \pm\kappa_2\}$, we can adopt the union bound of SPER to evaluate the proposed PANC scheme as (37).

For power scaling factor, we observe that the coefficients α we develop is independent of the detailed modulation schemes. Through some straightforward algebra, it is easy to show that our virtual channel model still fits for higher-order modulations, i.e., the quality of source-relay channel and source-destination channel are approximately characterized by the worst channel. Therefore, full diversity can be achieved by using the same power scaling scheme in the higher-order modulations.

For power adaptation factors optimization, we can optimize parameters $\tilde{\kappa}_1$ and $\tilde{\kappa}_2$ by solving the following optimization problem

$$\begin{aligned} &\min \sum_{i,j\in[1,16],i\neq j} P_{(T_i\to T_j)}\left(\tilde{\kappa}_1,\tilde{\kappa}_2\right) \\ &s.t.\ \ \tilde{\kappa}_1^2+\tilde{\kappa}_2^2 \le 2E_{\mathcal{R}}^{ave}; \tilde{\kappa}_1,\tilde{\kappa}_2 \ge 0; \tilde{\kappa}_1 \ge \tilde{\kappa}_2. \end{aligned} \tag{38}$$

Alternatively, we can also adopt Euclidean distance optimization method to optimize parameters $\tilde{\kappa}_1$ and $\tilde{\kappa}_2$ as

$$\begin{aligned} &\max\ u \\ &s.t.\ \ -\overline{V_iV_j} \le -u; \\ &\quad \tilde{\kappa}_1^2+\tilde{\kappa}_2^2 \le 2E_{\mathcal{R}}^{ave}; \tilde{\kappa}_1,\tilde{\kappa}_2 \ge 0; \kappa_1 \ge \kappa_2, \end{aligned} \tag{39}$$

where $V_i = \left(\sqrt{E_1}|h_{1\mathcal{D}}|x_1 + \sqrt{E_2}|h_{2\mathcal{D}}|x_2, |h_{\mathcal{RD}}|x_{\mathcal{R}}\right)$ and $x_{\mathcal{R}}$ is the correct network coded signal at relay corresponding to sources' information (x_1, x_2).

VII. Simulation Results

In this section, we evaluate the performance of the proposed PANC scheme by simulations. Consider a two dimensional cartesian coordinate system, where nodes $\mathcal{S}_1$, $\mathcal{S}_2$ and $\mathcal{D}$ are located at $(0, \frac{\sqrt{3}}{3})$, $(0, -\frac{\sqrt{3}}{3})$, and $(1, 0)$, respectively. The relay is moving from the origin point $(0, 0)$ to $(1, 0)$ at X-axis. Throughout our simulations, we use the path loss model $\gamma_{ij} = d_{ij}^{-3}$, where γ_{ij} is the channel gain. The notation d_{ij} is the distance between two terminals, where $i \in \{\mathcal{S}_1, \mathcal{S}_2, \mathcal{R}\}$ and $j \in \{\mathcal{R}, \mathcal{D}\}$. We assume that $E_1 = E_2 = E_{\mathcal{R}}^{ave} = 1$, and the SNR in the simulation is defined as $\rho = E_1/\sigma^2$. The average SNR range is $[0, 30]$ dB. To simplify the legends of simulation results figures, 'sim' stands for Monte-Carlo simulation result, 'thy' stands for the theoretical results.

In order to investigate the performance of our proposed scheme comprehensively, we consider the relay placed at different locations, resulting in different channel scenarios. Firstly, we consider the relay is located at $(0, 0)$, so the relay is close to the sources, i.e., forming an asymmetric network with strong source-relay channel, shown in Fig. 6. Then, we consider the relay is located at $(\frac{1}{3}, 0)$, so the distance between the source and relay is equal to the distance between the relay and destination, i.e., forming a symmetric network, shown in Fig. 7. Finally, we consider the relay is located at $(0.8, 0)$, so the distance between the sources and relay is larger than the distance between the relay to destination, i.e., forming an asymmetric network with a strong relay-destination channel, shown in Fig. 8.

In each realization of nodes locations, we evaluate the performance of the proposed PANC scheme as follows: (a) the SPER performance of the original received constellation with optimized $\tilde{\kappa}_1$ and $\tilde{\kappa}_2$ given in (34) by monte carlo simulation, denoted by *Origin-sim*; (b) the SPER performance of the received constellation after a coordinate transformation with optimized $\tilde{\kappa}_1$ and $\tilde{\kappa}_2$ given in (34) by both monte carlo simulation and theoretical expressions, denoted by *CT-sim* and *CT-thy*, respectively.

As the references, we simulate the following schemes: (a) the SPER performance of the CXNC scheme [7, 33] in which the relay transmits an XORed signal to the destination in the second transmission phase, denoted by *CXNC*; (b) the SPER performance of the CXNC scheme in which the relay transmits a power scaled XORed signal to the destination in the second transmission phase, denoted by *CXNC*$_\alpha$; (c) the

$$SPER \leq \left\{ \sum_{i,j\in\{1,\cdots,4\},i\neq j} \sum_{m,n\in\{\pm\kappa_1,\pm\kappa_2\}} P\left(T_j \left| \sqrt{E_R}x_R = m + in, T_i, h_{1D}, h_{2D}, h_{RD}\right.\right) P\left(\sqrt{E_R}x_R = m + in \left| T_i, h_{1R}, h_{2R}\right.\right)\right\}. \tag{37}$$

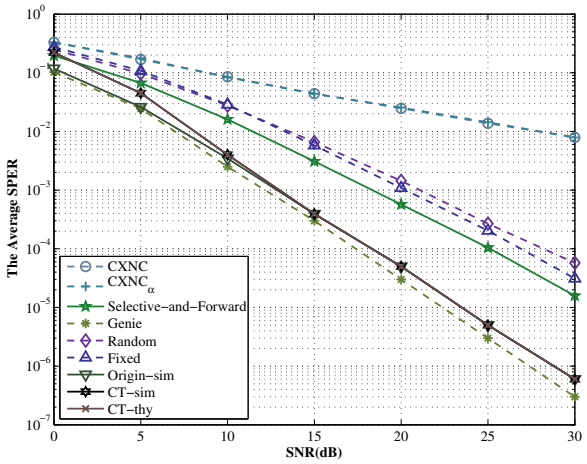

Fig. 6. Error performance with strong source-relay channel.

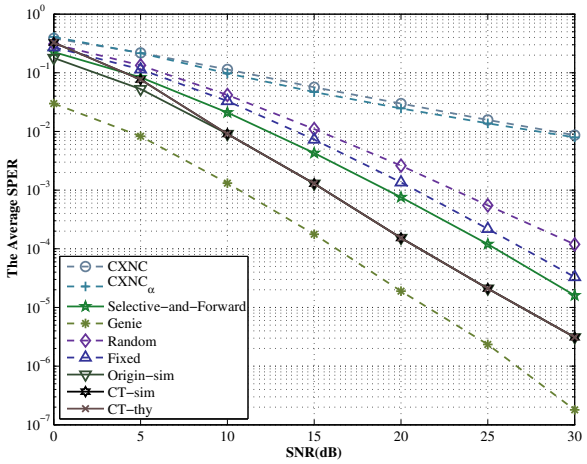

Fig. 8. Error performance with strong relay-destination channel.

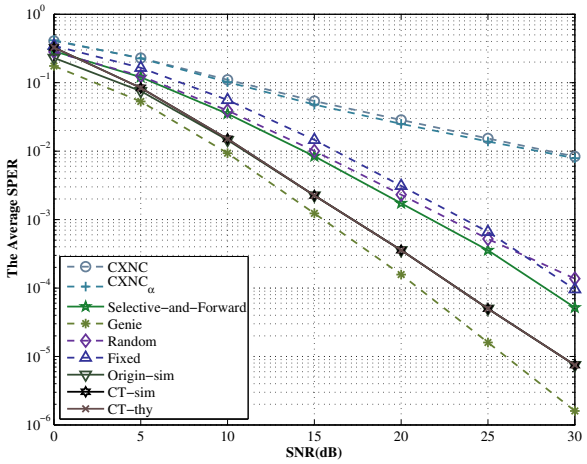

Fig. 7. Error performance in a symmetric network.

SPER performance of a selective-and-forward network coding scheme based on [20], denoted by *Selective-and-Forward*; (d) the SPER performance of a genie-aided PANC scheme, under the hypothetical assumption that the symbols are perfectly detected at the relay and both $\tilde{\kappa}_1$ and $\tilde{\kappa}_2$ are optimized by (34), denoted by *Genie*; (e) the SPER performance of the PANC scheme with randomly generated $\tilde{\kappa}_1$ and $\tilde{\kappa}_2$, in which $\tilde{\kappa}_1$ is a uniformly distributed random variable between $[1, \sqrt{2}]$ and $\tilde{\kappa}_2 = \sqrt{2E_{\mathcal{R}}^{ave} - \tilde{\kappa}_1^2}$. Both $\tilde{\kappa}_1$ and $\tilde{\kappa}_2$ are regenerated in different transmission periods, denoted by *Random*; and (f) the SPER performance of the PANC scheme with randomly generated $\tilde{\kappa}_1$ and $\tilde{\kappa}_2$, in which $\tilde{\kappa}_1 = 3\tilde{\kappa}_2 = 3/\sqrt{5}$. Both $\tilde{\kappa}_1$ and $\tilde{\kappa}_2$ are fixed in all the transmissions, denoted by *Fixed*.

Firstly, the CXNC without power scaling can only achieve a diversity of one, due to the error propagation from the source-relay hop as *Theorem 1* indicates. The CXNC with power scaling still cannot achieve a full diversity due to the multi-user interference of non-orthogonal MARC as *Theorem 2* infers. The proposed PANC scheme with a power scaling factor can achieve a full diversity no matter what power levels it adopts at the relay, which verify the proof of *Theorem 2*. The *Genie* method serves as the benchmark of the system performance, since it assumes that a genie exists at the relay and guarantees that the relay transmits correct information to the destination. We can conclude from the simulation results that the PANC scheme with the proposed design of allocating different power levels and adopting a power scaling factor can achieve full diversity in a MARC system.

In addition, the SPER performance based on a new coordinate system is larger than the SPER based on the original coordinate system for low SNR (e.g., from 0dB to 5dB), and coincides after 10dB. The reason for such phenomenon is that the detector based on the new coordinate system is sub-optimal comparing to the optimal ML detection in (3). Thus, the error performance based on the new coordinate system is poorer than its counterpart based on the original coordinate. As the SNR increases, the minimum Euclidean distance between the constellation points in both original and new coordinates systems increases, so the error performances become perfectly matched. Note that the theoretical results of the transformed coordinate systems match the Monte-Carlo simulation results. This shows that the closed-form SPER expressions obtained by the CT methods are accurate.

Note that, allocating different power levels at the relay may vary the coding gain of the system. In particular, the SPER performance of optimized $\tilde{\kappa}_1$ and $\tilde{\kappa}_2$, based on the Euclidean distance optimization method, has the best coding gain for both original coordinate and CT case. The SPER performance

for random or fixed chosen $\tilde{\kappa}_1$ and $\tilde{\kappa}_2$ has a lower coding gain performance because they are not adaptive to the instantaneous CSI comparing with the optimized $\tilde{\kappa}_1$ and $\tilde{\kappa}_2$. Although the selective-and-forward network coding scheme can achieve full diversity, it has a lower coding gain comparing to the PANC scheme.

Since there exists error propagation from the source-relay hop to the destination, we notice that the gap between the SPER performance of a genie-aided PANC scheme and the SPER performance of the original received constellation with optimized $\tilde{\kappa}_1$ and $\tilde{\kappa}_2$ is different with three relay location realizations. In particular, such gap is quite small when we have a strong source-relay channel, and the gap grows as the relay moves further from the source and closer to the destination. The reason is that with a strong source-relay channel, the relay will generate more reliable information and thus reduces the influence of error propagation.

VIII. Conclusion

In this paper we propose a novel PANC scheme to achieve full diversity and a high coding gain for a non-orthogonal MARC. Firstly, we propose a coordinate transformation method to transform the parallelogram received constellation to a rectangle one at both relay and destination. Then we derive the approximate SPER based on the coordinate transformed constellation. Next, we discuss the derivation of optimal power levels by separately obtaining the power scaling factor and optimal power adaptation factors. In particular, by applying the power scaling factor at the relay, the proposed PANC scheme can achieve a full diversity. Also, we propose a Euclidean distance optimization problem to obtain the optimal power levels at the relay. Finally, simulation results show that the SPER expressions based on our method can well approximate the exact SPER with a much lower complexity, and our PANC scheme with power adaptation factors optimization and power scaling factor design can achieve a full diversity and a higher coding gain compared to other network coding schemes.

Appendix

A. Computations on Wedge Probability

The wedge probability computation method [23, 34] can be utilized to derive the SPER with irregular decision regions. In the following, we will discuss three wedge prototypes as shown in Fig. 9. Let us first review the wedges discussed in [34]. Let us denote a CP by V_i and a vertex of the wedge by M_k. We assume that the angle in the counter-clockwise direction is positive and in the clockwise direction is negative.

There are two types of wedge error probabilities to be considered when V_i is outside the wedge region. For $\phi_1\phi_2 \geq 0$ as presented in Fig. 9 (1), the wedge probability is given by [34]

$$P_{w_1}(d_{ik},\phi_1,\phi_2) = \frac{1}{2}\left\{Q_2\left(\sqrt{2d_{ik}}\sin\phi_2;\frac{\tan^2\phi_2-1}{\tan^2\phi_2+1}\right) - Q_2\left(\sqrt{2d_{ik}}\sin\phi_1;\frac{\tan^2\phi_1-1}{\tan^2\phi_1+1}\right)\right\}, \tag{40}$$

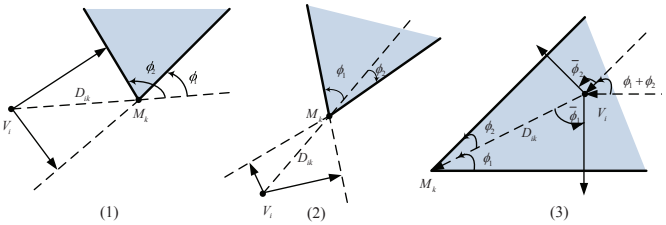

Fig. 9. Demonstrations for the basic patterns of wedge probabilities. d_{ik} (or d_{ij}) is the normalized distance between CP V_i and wedge vertex M_k (or M_j). In particular, both (1) and (2) are introduced in [34]. And in (3), ϕ_i with $i \in \{1,2\}$ are included angle between line V_iM_k and wedge sides; and $\phi_i + \bar{\phi}_i = \pi$.

where the two-dimensional Q-function $Q_2(x;\rho)$ is defined in the Notations, and its closed-form solution can be found in Eqs (5.74) on [35].

Similarly, for $\phi_1\phi_2 < 0$ as shown in Fig. 9 (2), the wedge error probability is given by [34]

$$P_{w_2}(d_{ik},\phi_1,\phi_2) = \frac{1}{2}\left\{Q_2\left(\sqrt{2d_{ik}}\sin\phi_1;\frac{\tan^2\phi_1-1}{\tan^2\phi_2+1}\right) - Q_2\left(\sqrt{2d_{ik}}\sin(-\phi_2);\frac{\tan^2\phi_2-1}{\tan^2\phi_1+1}\right)\right\}. \tag{41}$$

Next, we discuss the probability of correct decisions, i.e., the received signal is inside the decision region of V_i. We use two different ways to represent the probabilities corresponding to two different decision regions, as shown in Fig. 9 (4) and (5). In particular, the probability of a received signal within the wedge region with vertex M_k, shown in Fig. 9 (3), is given by

$$\begin{aligned} &P_{w_3}(d_{ik},\phi_1,\phi_2) \\ &= \frac{1}{2\pi}\sum_{n=1}^{2}\left(1-\int_0^{\bar{\phi}_n}\exp\left(-\frac{d_{ik}\sin^2\phi_n}{\sin^2(\phi_n+\phi)}\right)d\phi\right)+\frac{\phi_1+\phi_2}{2\pi} \\ &= \frac{1}{2\pi}\sum_{n=1}^{2}\left(Q_2\left(\sqrt{2d_{ik}}\sin\phi_n;\frac{\tan^2\phi_n-1}{\tan^2\phi_n+1}\right)\right. \\ &\left.-\pi Q_1\left(\sqrt{2d_{ik}}\sin\phi_n\right)\right)+\frac{\phi_1+\phi_2+2}{2\pi}. \end{aligned} \tag{42}$$

B. Derivation of the coordinate transformation at the relay

Let us define $\mathbf{Z} = [\Re\{y_{\mathcal{R}}\}, \Im\{y_{\mathcal{R}}\}]^T$ as the point on the original coordinate, where $(\cdot)^T$ is the transform operation of the matrix or vector, 2×1 vector $\mathbf{Z}'$ as the intermediate transformed point, $\mathbf{A}$ as the intermediate coordinate transformation matrix. The relationship between $\mathbf{Z}$ and $\mathbf{Z}'$ is $\mathbf{Z} = \mathbf{A}\mathbf{Z}'$, where $\mathbf{A}$ is a 2×2 matrix and $\det(\mathbf{A}) \neq 0$. The probability density function of $\mathbf{Z}$ can be represented by $\mathbf{Z}'$ as

$$\begin{aligned} f_{\mathbf{Z}}(z) &= \frac{1}{2\pi|\Sigma|^{1/2}}\exp\left(-\frac{1}{2}(\mathbf{z}-\mathbf{V}_i)^T\Sigma^{-1}(\mathbf{z}-\mathbf{V}_i)\right) \\ &= \frac{1}{2\pi|\Sigma|^{1/2}}\exp\left(-\frac{1}{2}(\mathbf{z}'-\mathbf{A}^{-1}\mathbf{V}_i)^T\mathbf{A}^T\Sigma^{-1}\mathbf{A}(\mathbf{z}'-\mathbf{A}^{-1}\mathbf{V}_i)\right), \end{aligned} \tag{43}$$

where $\Sigma = [\sigma^2/2, 0; 0, \sigma^2/2]$, and $|\Sigma|$ is the determinant of Σ, $i \in \{1,\cdots,4\}$. Note that the covariance matrix $\mathbf{B} \triangleq \mathbf{A}^T\Sigma^{-1}\mathbf{A}$ is not diagonal. We apply the eigenvalue

decomposition to $\mathbf{B}$ and obtain

$$f_{\mathbf{Z}}(z) = \frac{1}{2\pi|\Sigma|^{1/2}} \exp\left(-\frac{1}{2}(\mathbf{z}' - \mathbf{A}^{-1}\mathbf{V}_i^T)^T[\psi_1,\psi_2]^T \begin{bmatrix} \lambda_1 & 0 \\ 0 & \lambda_2 \end{bmatrix} [\psi_1,\psi_2](\mathbf{z}' - \mathbf{A}^{-1}\mathbf{V}_i^T)\right), \tag{44}$$

where ψ_i for $i = 1, 2$ and λ_i are the eigenvectors and eigenvalues of $\mathbf{B}$, respectively. Thus, we define $\overline{\mathbf{Z}} = [\psi_1, \psi_2](\mathbf{z}' - \mathbf{A}^{-1}\mathbf{V}_i^T)$, which is a complex Gaussian random variable with the mean $\overline{\mathbf{V}}_i = [\psi_1, \psi_2]\mathbf{A}^{-1}\mathbf{V}_i^T$ and covariance $[\lambda_1, 0; 0, \lambda_2]$, as the point on the transformed coordinate. Let $\mathbf{Q} = [\psi_1, \psi_2]$, the relationship between the original received signal $\mathbf{Z}$ and the transformed received signal $\overline{\mathbf{Z}}$, the original RP $\mathbf{V}_i$ and the transformed RP $\overline{\mathbf{V}}_i$ after the coordinate transformation and decorrelation are

$$\overline{\mathbf{Z}} = \mathbf{Q}\mathbf{A}^{-1}\mathbf{Z} \text{ and } \overline{\mathbf{V}}_i = \mathbf{Q}\mathbf{A}^{-1}\mathbf{V}_i^T, \tag{45}$$

respectively. To transform the RP-composed parallelogram to a rectangle centered at the origin point and preserve the length of the geometry's sides, e.g., $\overrightarrow{\overline{V}_i\overline{V}_j} = \overrightarrow{V_iV_j}$, the transformation matrix $\mathbf{A}$ is given by

$$\begin{aligned}\mathbf{A} &= \begin{bmatrix} \overrightarrow{V_1V_2} & -\overrightarrow{V_1V_2} \\ \overrightarrow{V_1V_3} & \overrightarrow{V_1V_3} \end{bmatrix} \begin{bmatrix} \mathbf{V}_1(1) & \mathbf{V}_2(1) \\ \mathbf{V}_1(2) & \mathbf{V}_2(2) \end{bmatrix}^{-1} \\ &= \frac{2}{\beta} \begin{bmatrix} |h_{1\mathcal{R}}|\Im\{h_{2\mathcal{R}}\} & -|h_{1\mathcal{R}}|\Re\{h_{2\mathcal{R}}\} \\ -|h_{2\mathcal{R}}|\Im\{h_{1\mathcal{R}}\} & |h_{2\mathcal{R}}|\Re\{h_{1\mathcal{R}}\} \end{bmatrix},\end{aligned} \tag{46}$$

where $\beta = \Re\{h_{1\mathcal{R}}\}\Im\{h_{2\mathcal{R}}\} - \Re\{h_{2\mathcal{R}}\}\Im\{h_{1\mathcal{R}}\}$ and matrix $\mathbf{B}$ shown in (47). For $i = 1, 2$, the eigenvalues are given by (48). From (47) and (48) we can see that $\mathbf{B}$ is a real orthogonal symmetric matrix. In this case, matrix $\mathbf{Q}$ is a rotation matrix. Hence, the coordinate transformed by $\mathbf{A}$ is a rectangle with its sides parallel to the axis, and after the eigenvalue decomposition, the new constellation is still a rectangle and being rotated counterclockwise through an angle θ, which is defined by $\mathbf{Q} = [\cos(\theta), \sin(\theta); -\sin(\theta), \cos(\theta)]^T$. The corresponding eigenvectors matrix is given by (18). In this case, the final coordinate transform matrix $\mathbf{C}$ is given by

$$\mathbf{C} = \mathbf{Q}\mathbf{A}^{-1}, \tag{49}$$

where $\mathbf{A}^{-1}$ is shown in (18).

C. Proof of Theorem 1

Firstly, we consider the case that T_1 is wrongly decoded in to other symbol pairs. The average probability that T_1 is wrongly decoded into T_4 at the destination is given by (50).

Without loss of generality, we assume $E_1 = E_2 = E_{\mathcal{R}} = E$ in the following. Let us define $\rho = E/\sigma^2$ as the reference system SNR for $i \in \{1, 2, \mathcal{R}\}$. In general, averaging the following one-dimensional Q-function over channel distributions, we have

$$\mathbb{E}\left\{Q_1\left(\sqrt{2\rho|h_{ij}|^2}\right)\right\} = \frac{1}{\pi}\int_0^{\pi/2}\left(1 + \frac{\rho\gamma_{ij}}{\sin^2\theta}\right)^{-1} d\theta \overset{\rho\to\infty}{\approx} \frac{1}{4\gamma_{ij}}\rho^{-1}. \tag{51}$$

Likewise, $\mathbb{E}\left\{Q_1\left(\sqrt{2\rho\sum_{t\in\{ij,mn\}}|h_t|^2}\right)\right\} \overset{\rho\to\infty}{\approx} \frac{3}{16\gamma_{ij}\gamma_{mn}}\rho^{-2}$ and $\mathbb{E}\{Q_1(\sqrt{2\rho\sum_{t\in\{ij,mn,pq\}}|h_t|^2})\} \overset{\rho\to\infty}{\approx} \frac{5}{32\gamma_{ij}\gamma_{mn}\gamma_{pq}}\rho^{-3}$. According to the result in [36], we have the high-SNR approximation

$$\begin{aligned}&\mathbb{E}\left\{Q_1\left[\frac{\sqrt{2}\left(\left(\sum_{i=1}^2\sqrt{E_i}|h_{i\mathcal{D}}|\right)^2 - |h_{\mathcal{R}\mathcal{D}}|^2\kappa_1\kappa_2\right)}{\sqrt{(E_1|h_{1\mathcal{D}}|^2 + E_2|h_{2\mathcal{D}}|^2 + |h_{\mathcal{R}\mathcal{D}}|^2\kappa_1^2)\,\sigma^2}}\right]\right\} \\ &\approx \frac{\gamma_{\mathcal{R}\mathcal{D}}}{\gamma_{1\mathcal{D}} + \gamma_{2\mathcal{D}} + \gamma_{\mathcal{R}\mathcal{D}}}.\end{aligned} \tag{52}$$

With the approximations in (51) and (52), averaging the probability $P(T_1 \to T_4|\mathbf{h})$ in (50) over channel distributions, we further have

$$\begin{aligned}P(T_1 \to T_4) \approx{}& \frac{5}{32\gamma_{1\mathcal{D}}\gamma_{2\mathcal{D}}\gamma_{\mathcal{R}\mathcal{D}}}\rho^{-3} + \frac{5}{128\gamma_{1\mathcal{D}}\gamma_{2\mathcal{D}}\gamma_{\mathcal{R}\mathcal{D}}\gamma_{1\mathcal{R}}}\rho^{-4} \\ &+ \frac{\gamma_{\mathcal{R}\mathcal{D}}}{4\gamma_{2\mathcal{R}}(\gamma_{1\mathcal{D}} + \gamma_{2\mathcal{D}} + \gamma_{\mathcal{R}\mathcal{D}})}\rho^{-1} \\ &+ \frac{\gamma_{\mathcal{R}\mathcal{D}}}{4\gamma_{12\mathcal{R}}(\gamma_{1\mathcal{D}} + \gamma_{2\mathcal{D}} + \gamma_{\mathcal{R}\mathcal{D}})}\rho^{-1},\end{aligned} \tag{53}$$

where $\gamma_{12\mathcal{R}} = \gamma_{1\mathcal{R}} + \gamma_{2\mathcal{R}}$. Likewise, we can derive $P(T_2 \to T_3)$.

When only one error occurs, we further have (54). Similarly, we can derive $P(T_1 \to T_3)$, $P(T_2 \to T_4)$. From (53) and (54), we conclude that the PANC scheme can only achieve the diversity of one in a MARC system without power scaling. In the NC based MARC, averaging the related PEPs over the channel coefficients, we have

$$\begin{aligned}P(T_1 \to T_4) \approx{}& \frac{5}{32\gamma_{12\mathcal{D}}\gamma_{\mathcal{R}\mathcal{D}}\gamma_{1\mathcal{R}}}\rho^{-3} \\ &+ \frac{5}{32\gamma_{12\mathcal{D}}\gamma_{\mathcal{R}\mathcal{D}}\gamma_{2\mathcal{R}}}\rho^{-3} + \frac{1}{4\gamma_{12\mathcal{D}}}\rho^{-1}, \\ P(T_1 \to T_2) \approx{}& \frac{3}{16\gamma_{1\mathcal{D}}\gamma_{1\mathcal{R}}}\rho^{-2} \\ &+ \frac{3}{16\gamma_{1\mathcal{D}}\gamma_{2\mathcal{R}}}\rho^{-2} + \frac{3}{16\gamma_{1\mathcal{D}}\gamma_{\mathcal{R}\mathcal{D}}}\rho^{-2}.\end{aligned} \tag{55}$$

where $\gamma_{12\mathcal{D}} = \gamma_{1\mathcal{D}} + \gamma_{2\mathcal{D}}$. Similarly, we can derive $P(T_1 \to T_3)$, $P(T_2 \to T_3)$ and $P(T_2 \to T_4)$. In this case, we can conclude that the MARC system with network coding cannot achieve full diversity.

D. Proof of Theorem 2

We prove *Theorem 2* by using our virtual channel model. After some manipulations, it is easy to show that given any power scaling coefficient α employed at the relay side, the lower bound of the SPER can be in general approximated as (56).

After applying the Chernoff bound $Q_1(x) \le \frac{1}{2}\exp\left(-\frac{x^2}{2}\right)$, we can further obtain (57), where Λ_i, r are the ith non-zero eigenvalue and the rank of the diagonal matrix $[\frac{(\sqrt{E_1}|h_{1\mathcal{D}}|(x_1-\hat{x}_1)+\sqrt{E_2}|h_{2\mathcal{D}}|(x_2-\hat{x}_2))^2}{4}, 0; 0, \frac{\gamma_{\mathcal{S}\mathcal{R}\mathcal{D}}(x_{\mathcal{R}}-\hat{x}_{\mathcal{R}})^2}{4}]$, respectively. $\gamma_{\mathcal{S}\mathcal{R}\mathcal{D}} = \min\{\gamma_{\mathcal{S}\mathcal{R}}, \gamma_{\mathcal{R}\mathcal{D}}\}$ is an exponential distributed random variable with the mean $\frac{\gamma_{1\mathcal{R}}\gamma_{2\mathcal{R}}\gamma_{\mathcal{R}\mathcal{D}}}{\gamma_{1\mathcal{R}}\gamma_{2\mathcal{R}}+\gamma_{1\mathcal{R}}\gamma_{\mathcal{R}\mathcal{D}}+\gamma_{2\mathcal{R}}\gamma_{\mathcal{R}\mathcal{D}}}$, which is proven as follows. Let us define $T = \min(E_1|h_{1\mathcal{R}}|^2, E_2|h_{2\mathcal{R}}|^2)$. Since $\gamma_{\mathcal{S}\mathcal{R}\mathcal{D}} =$

$$\mathbf{B}=\frac{4}{\beta\sigma^2}\left[\begin{array}{cc}|h_{1\mathcal{R}}|^2\Im^2\{h_{2\mathcal{R}}\}+|h_{2\mathcal{R}}|^2\Im^2\{h_{1\mathcal{R}}\} & -|h_{1\mathcal{R}}|^2\Re\{h_{2\mathcal{R}}\}\Im\{h_{2\mathcal{R}}\}-|h_{2\mathcal{R}}|^2\Re\{h_{1\mathcal{R}}\}\Im\{h_{1\mathcal{R}}\}\\ -|h_{1\mathcal{R}}|^2\Re\{h_{2\mathcal{R}}\}\Im\{h_{2\mathcal{R}}\}-|h_{2\mathcal{R}}|^2\Re\{h_{1\mathcal{R}}\}\Im\{h_{1\mathcal{R}}\} & |h_{1\mathcal{R}}|^2\Re^2\{h_{2\mathcal{R}}\}+|h_{2\mathcal{R}}|^2\Re^2\{h_{1\mathcal{R}}\}\end{array}\right]. \tag{47}$$

$$\lambda_i=\frac{\mathbf{B}(1,1)+\mathbf{B}(2,2)\pm\sqrt{\mathbf{B}(1,1)^2+\mathbf{B}(2,2)^2+4\mathbf{B}(1,2)^2-2\mathbf{B}(1,1)\mathbf{B}(2,2)}}{2}. \tag{48}$$

$$\begin{aligned}
&P(T_1\to T_4)=\mathbb{E}\{P(T_1\to T_4|\mathbf{h})\}\\
&=\mathbb{E}\left\{\sum_{k\in\{\pm\kappa_1,\pm\kappa_2\}}P(T_1\to T_4|\sqrt{E_{\mathcal{R}}}x_{\mathcal{R}}=k,T_1,h_{1\mathcal{D}},h_{2\mathcal{D}},h_{\mathcal{RD}})P(\sqrt{E_{\mathcal{R}}}x_{\mathcal{R}}=k|T_1,h_{1\mathcal{R}},h_{2\mathcal{R}})\right\}\\
&=\mathbb{E}\left\{Q_1\left[\frac{\sqrt{2}\left(\left(\sum_{i=1}^2\sqrt{E_i}|h_{i\mathcal{D}}|\right)^2+|h_{\mathcal{RD}}|^2\kappa_1^2\right)}{\sqrt{\left(E_1|h_{1\mathcal{D}}|^2+E_2|h_{2\mathcal{D}}|^2+|h_{\mathcal{RD}}|^2\kappa_1^2\right)\sigma^2}}\right]\left[1-\sum_{i=1}^2Q_1\left(\sqrt{2\left(E_i|h_{i\mathcal{R}}|^2/\sigma^2\right)}\right)\right.\right.\\
&\left.-Q_1\left(\sqrt{2\left(\sum_{i=1}^2\sqrt{E_i}h_{i\mathcal{R}}\right)^2/\sigma^2}\right)\right]+Q_1\left[\frac{\sqrt{2}\left(\left(\sum_{i=1}^2\sqrt{E_i}|h_{i\mathcal{D}}|\right)^2+|h_{\mathcal{RD}}|^2\kappa_1\kappa_2\right)}{\sqrt{\left(E_1|h_{1\mathcal{D}}|^2+E_2|h_{2\mathcal{D}}|^2+|h_{\mathcal{RD}}|^2\kappa_1^2\right)\sigma^2}}\right]Q_1\left(\sqrt{2\left(E_1|h_{1\mathcal{R}}|^2/\sigma^2\right)}\right)\\
&+Q_1\left[\frac{\sqrt{2}\left(\left(\sum_{i=1}^2\sqrt{E_i}|h_{i\mathcal{D}}|\right)^2-|h_{\mathcal{RD}}|^2\kappa_1\kappa_2\right)}{\sqrt{\left(E_1|h_{1\mathcal{D}}|^2+E_2|h_{2\mathcal{D}}|^2+|h_{\mathcal{RD}}|^2\kappa_1^2\right)\sigma^2}}\right]Q_1\left(\sqrt{2\left(E_2|h_{2\mathcal{R}}|^2/\sigma^2\right)}\right)\\
&\left.+Q_1\left[\frac{\sqrt{2}\left(\left(\sum_{i=1}^2\sqrt{E_i}|h_{i\mathcal{D}}|\right)^2-|h_{\mathcal{RD}}|^2\kappa_1^2\right)}{\sqrt{\left(E_1|h_{1\mathcal{D}}|^2+E_2|h_{2\mathcal{D}}|^2+|h_{\mathcal{RD}}|^2\kappa_1^2\right)\sigma^2}}\right]Q_1\left(\sqrt{2\left(\sum_{i=1}^2\sqrt{E_i}h_{i\mathcal{R}}\right)^2/\sigma^2}\right)\right\}.
\end{aligned} \tag{50}$$

$$P(T_1\to T_2)\approx\left\{\begin{array}{ll}\frac{3}{16\gamma_{1\mathcal{D}}\gamma_{\mathcal{RD}}}\rho^{-2}+\frac{1}{4\gamma_{1\mathcal{R}}}\rho^{-1}+\frac{1}{4\gamma_{2\mathcal{R}}}\rho^{-1}+\frac{1}{4\gamma_{12\mathcal{R}}}\rho^{-1}, & \text{when } \kappa_1>\kappa_2,\\ \frac{3}{16\gamma_{1\mathcal{D}}\gamma_{\mathcal{RD}}}\rho^{-2}+\frac{1}{4\gamma_{1\mathcal{R}}}\rho^{-1}+\frac{3}{64\gamma_{1\mathcal{D}}\gamma_{\mathcal{RD}}\gamma_{2\mathcal{R}}}\rho^{-3}+\frac{3}{64\gamma_{1\mathcal{D}}\gamma_{\mathcal{RD}}\gamma_{12\mathcal{R}}}\rho^{-3}, & \text{when } \kappa_1<\kappa_2,\\ \frac{3}{16\gamma_{1\mathcal{D}}\gamma_{\mathcal{RD}}}\rho^{-2}+\frac{1}{4\gamma_{1\mathcal{R}}}\rho^{-1}+\frac{1}{16\gamma_{1\mathcal{D}}\gamma_{2\mathcal{R}}}\rho^{-2}+\frac{1}{16\gamma_{1\mathcal{D}}\gamma_{12\mathcal{R}}}\rho^{-2}, & \text{when } \kappa_1=\kappa_2.\end{array}\right. \tag{54}$$

$$\begin{aligned}
P_v&\triangleq P\left((x_1,x_2,x_{\mathcal{R}})\to(\hat{x}_1,\hat{x}_2,\hat{x}_{\mathcal{R}})\right)\\
&=\mathbb{E}\left[Q\left(\frac{\left(\sqrt{E_1}|h_{1\mathcal{D}}|\left(x_1-\hat{x}_1\right)+\sqrt{E_2}|h_{2\mathcal{D}}|\left(x_2-\hat{x}_2\right)\right)^2+\alpha|h_{\mathcal{RD}}|^2(x_{\mathcal{R}}-\hat{x}_{\mathcal{R}})^2}{\sqrt{E_1|h_{1\mathcal{D}}|^2(x_1-\hat{x}_1)^2+E_2|h_{2\mathcal{D}}|^2(x_2-\hat{x}_2)^2+\alpha|h_{\mathcal{RD}}|^2(x_{\mathcal{R}}-\hat{x}_{\mathcal{R}})^2}}\right)\right]\\
&\overset{(x+y)^2\le 2\left(x^2+y^2\right)}{\le}\mathbb{E}\left[Q\left(\frac{\left(\sqrt{E_1}|h_{1\mathcal{D}}|\left(x_1-\hat{x}_1\right)+\sqrt{E_2}|h_{2\mathcal{D}}|\left(x_2-\hat{x}_2\right)\right)^2+\alpha|h_{\mathcal{RD}}|^2(x_{\mathcal{R}}-\hat{x}_{\mathcal{R}})^2}{2\sqrt{\left(\sqrt{E_1}|h_{1\mathcal{D}}|(x_1-\hat{x}_1)+\sqrt{E_2}|h_{2\mathcal{D}}|(x_2-\hat{x}_2)\right)^2+\alpha|h_{\mathcal{RD}}|^2(x_{\mathcal{R}}-\hat{x}_{\mathcal{R}})^2}}\right)\right].
\end{aligned} \tag{56}$$

$$P_v\le\mathbb{E}\left[\frac{1}{2}\exp\left(-\frac{\left(\sqrt{E_1}|h_{1\mathcal{D}}|(x_1-\hat{x}_1)+\sqrt{E_2}|h_{2\mathcal{D}}|(x_2-\hat{x}_2)\right)^2+\gamma_{\mathcal{SRD}}|x_{\mathcal{R}}-\hat{x}_{\mathcal{R}}|^2}{4}\right)\right]\overset{\rho\to\infty}{\approx}\frac{1}{2}\left(\prod_{k=1}^r\Lambda_i\right)^{-1}\rho^{-r} \tag{57}$$

$$P\left((x_1,x_2,x_{\mathcal{R}})\to(-\hat{x}_1,\hat{x}_2,\hat{x}_{\mathcal{R}})\right)\approx\mathbb{E}\left[Q\left(\frac{2E_1|h_{1\mathcal{D}}|^2}{\sqrt{E_1|h_{1\mathcal{D}}|^2(x_1-\hat{x}_1)^2+E_2|h_{2\mathcal{D}}|^2(x_2-\hat{x}_2)^2+\alpha|h_{\mathcal{RD}}|^2(x_{\mathcal{R}}-\hat{x}_{\mathcal{R}})^2}}\right)\right]. \tag{58}$$

$\min\{E_1|h_{1\mathcal{R}}|^2,E_2|h_{2\mathcal{R}}|^2,(\sqrt{E_1}|h_{1\mathcal{R}}|+\sqrt{E_2}|h_{2\mathcal{R}}|)^2,\gamma_{\mathcal{RD}}\}$, we have

$$\begin{aligned}
2\gamma_{\mathcal{SRD}}&\ge\min\{2E_1|h_{1\mathcal{R}}|^2,2E_2|h_{2\mathcal{R}}|^2,\sum_{i=1}^2E_i|h_{i\mathcal{R}}|^2,2\gamma_{\mathcal{RD}}\}\\
&\ge 2\min\{T,\gamma_{\mathcal{RD}}\}.
\end{aligned} \tag{59}$$

Because if X and Y are i.i.d. exponentially distributed random variables with the mean v_x and v_y, respectively, $\min\{X,Y\}$ is a also an exponentially distributed random variable with the mean v_x+v_y. Hence, we have proved that $\gamma_{\mathcal{SRD}}$ is also an exponentially distributed random variable. Since both two diagonal elements are non-zero when an error event happens or two error events happen, we have $\max_{\hat{x}\neq x}\Pr\left(x\to\hat{x}\right)=\mathrm{O}\left(\Gamma^{-2}\right)$. Note that, replacing $\gamma_{\mathcal{RD}}$ in (57) by $\bar{\gamma}_{\mathcal{RD}}$ will not change the diversity value, which completes the proof of the theorem.

If we apply the power scaling on CXNC scheme, when one error occurs, i.e., $\hat{x}_i=-x_i$ for $i\in\{1,2\}$, we have (58).

Averaging the probability in (58) over channel distributions,

we further have

$$P\left((x_1, x_2, x_{\mathcal{R}}) \to (-\hat{x}_1, \hat{x}_2, \hat{x}_{\mathcal{R}})\right) \approx \frac{1}{4\gamma_{1\mathcal{D}}}\rho^{-1}. \quad (60)$$

Hence, we can conclude that the power scaled CXNC scheme still cannot achieve the full diversity.

REFERENCES

[1] T. Cover and A. Gamal, "Capacity theorems for the relay channel," *IEEE Trans. Inf. Theory*, vol. 25, no. 5, pp. 572–584, Sep. 1979.

[2] J. N. Laneman, D. N. C. Tse, and G. W. Wornell, "Cooperative diversity in wireless networks: efficient protocols and outage behavior," *IEEE Trans. Inf. Theory*, vol. 50, no. 12, pp. 3062–3080, Dec. 2004.

[3] R. Ahlswede, N. Cai, S. Y. R. Li, and R. Yeung, "Network information flow," *IEEE Trans. Inf. Theory*, vol. 46, no. 4, pp. 1204–1216, Jul. 2000.

[4] S. Y. R. Li, R. W. Yeung, and N. Cai, "Linear network coding," *IEEE Trans. Inf. Theory*, vol. 49, no. 2, pp. 371–381, Feb. 2003.

[5] S. Katti, H. Rahul, W. Hu, D. Katabi, M. Medard, and J. Crowcroft, "Xors in the air: practical wireless network coding," in *Proc. 2006 ACM SIGCOMM*, pp. 243–254.

[6] T. Cui, T. Ho, and J. Kliewer, "Memoryless relay strategies for two-way relay channels," *IEEE Trans. Commun.*, vol. 57, no. 10, pp. 3132–3143, Oct. 2009.

[7] S. Zhang and S. C. Liew, "Channel coding and decoding in a relay system operated with physical-layer network coding," *IEEE J. Sel. Areas Commun.*, vol. 27, no. 5, pp. 788–796, Jun. 2009.

[8] T. Koike-Akino, P. Popovski, and V. Tarokh, "Optimized constellations for two-way wireless relaying with physical network coding," *IEEE J. Sel. Areas Commun.*, vol. 27, no. 5, pp. 773–787, Jun. 2009.

[9] L. Wei and W. Chen, "Efficient compute-and-forward network codes search for two-way relay channels," *IEEE Commun. Lett.*, vol. 16, no. 8, pp. 1204–1207, Aug. 2012.

[10] K. S. Gomadam and S. A. Jafar, "Optimal relay functionality for snr maximization in memoryless relay networks," *IEEE J. Sel. Areas Commun.*, vol. 25, no. 2, pp. 390–401, Feb. 2007.

[11] G. Kramer, M. Gastpar, and P. Gupta, "Cooperative strategies and capacity theorems for relay networks," *IEEE Trans. Inf. Theory*, vol. 51, no. 9, pp. 3037–3063, Sep. 2005.

[12] X. Bao and J. Li, "Adaptive network coded cooperation (ANCC) for wireless relay networks: matching code-on-graph with network-on-graph," *IEEE Trans. Wireless Commun.*, vol. 7, no. 2, pp. 574–583, Feb. 2008.

[13] J. Du, M. Xiao, and M. Skoglund, "Cooperative network coding strategies for wireless relay networks with backhaul," *IEEE Trans. Commun.*, vol. 59, no. 9, pp. 2502–2514, Sep. 2011.

[14] W. Guan and K. J. R. Liu, "Mitigating error propagation for wireless network coding," *IEEE Trans. Wireless Commun.*, vol. 11, no. 10, pp. 3632–3643, Oct. 2012.

[15] M. Xiao and M. Skoglund, "Multiple-user cooperative communications based on linear network coding," *IEEE Trans. Commun.*, vol. 58, no. 12, pp. 3345–3351, Dec. 2010.

[16] J. Li, J. Yuan, R. Malancy, M. Xiao, and W. Chen, "Full-diversity binary frame-wise network coding for multiple-source multiple-relay networks over slow-fading channels," *IEEE Trans. Veh. Technol.*, vol. 61, no. 3, pp. 1346–1360, Mar. 2012.

[17] J. Li, J. Yuan, R. Malaney, M. Azmi, and M. Xiao, "Network coded LDPC code design for a multi-source relaying system," *IEEE Trans. Wireless Commun.*, vol. 10, no. 5, pp. 1538–1551, May 2011.

[18] J. Li, W. Chen, Z. Lin, and B. Vucetic, "Design of physical layer network coded LDPC code for a multiple-access relaying system," *IEEE Commun. Lett.*, vol. 17, no. 4, pp. 749–752, Apr. 2013.

[19] M. Xiao and T. Aulin, "Optimal decoding and performance analysis of a noisy channel network with network coding," *IEEE Trans. Wireless Commun.*, vol. 57, no. 5, pp. 1402–1412, May 2009.

[20] M. Xiao, J. Kliewer, and M. Skoglund, "Design of network codes for multiple-user multiple-relay wireless networks," *IEEE Trans. Commun.*, vol. 60, no. 12, pp. 3755–3766, Dec. 2012.

[21] L. Wei and W. Chen, "Compute-and-forward network coding design over multi-source multi-relay channels," *IEEE Trans. Wireless Commun.*, vol. 11, no. 9, pp. 3348–3357, Sep. 2012.

[22] S. Wei, J. Li, and H. Su, "Joint orthogonal coding and modulation scheme for soft information in bi-directional networks," in *Proc. 2011 International Conference on WiCOM*, pp. 1–4.

[23] J. Craig, "A new, simple and exact result for calculating the probability of error for two-dimensional signal constellations," in *Proc. 1991 IEEE Military Communications Conference*, vol. 2, pp. 571–575.

[24] D. R. Brown III and P. H. V., "Time-slotted round-trip carrier synchronization for distributed beam forming," *IEEE Trans. Signal Process.*, vol. 56, no. 11, pp. 5630–5643, Nov. 2008.

[25] S. Berger and A. Wittneben, "Impact of noisy carrier phase synchronization on linear amplify-and-forward relaying," in *2007 IEEE Global Communications Conference.*

[26] S. Verdu, *Multiuser Detection*. Cambridge University Press, 1998.

[27] S. Wei, J. Li, W. Chen, and H. Su, "Wireless adaptive network coding strategy in multiple-access relay channels," in *Proc. 2012 IEEE International Conference on Communications*, vol. 9, pp. 4589–4594.

[28] L. Zheng and D. N. C. Tse, "Diversity and multiplexing: a fundamental tradeoff in multiple-antenna channels," *IEEE Trans. Inf. Theory*, vol. 49, no. 5, pp. 1073–1096, May 2003.

[29] T. Wang, G. Giannakis, and R. Wang, "Smart regenerative relays for link-adaptive cooperative communications," *IEEE Trans. Commun.*, vol. 56, no. 11, pp. 1950–1960, Nov. 2008.

[30] A. Nasri, R. Schober, and M. Uysal, "Performance and optimization of network-coded cooperative diversity systems," *IEEE Trans. Commun.*, vol. 61, no. 3, pp. 1111–1122, 2013.

[31] D. J. Love and R. W. Heath, "Limited feedback unitary precoding for spatial multiplexing systems," *IEEE Trans. Inf. Theory*, vol. 51, pp. 2967–2976, Aug. 2005.

[32] A. Roumy and D. Declercq, "Characterization and optimization of LDPC codes for the 2-user Gaussian multiple access channel," *EURASIP J. Wireless Commun. and Networking*, vol. 2007:074890, Jun. 2007.

[33] P. Popovski and H. Yomo, "The anti-packets can increase the achievable throughput of a wireless multi-hop network," in *Proc. 2006 IEEE International Conference on Communication*, vol. 9, pp. 3885–3890.

[34] A. Y. C. Peng, S. Yousefi, and I.-M. Kim, "On error analysis and distributed phase steering for wireless network coding over fading channels," *IEEE Trans. Wireless Commun.*, vol. 8, no. 11, pp. 5639–5649, Nov. 2009.

[35] M. K. Simon and M. S. Alouini, *Digital Communication over Fading Channels*. Wiley-IEEE Press, 2004.

[36] F. A. Onat, A. Adinoyi, F. Y., H. Yanikomeroglu, J. S. Thompson, and M. I. D., "Threshold selection for SNR-based selective relaying in cooperative wireless networks," *IEEE Trans. Wireless Commun.*, vol. 7, no. 11, pp. 4226–4237, Nov. 2008.

Sha Wei received the B.S. and M.S. degrees in Electronic engineering from the University of Electronic Science and Technology of China (UESTC), Chengdu, and Shanghai Jiao Tong University, Shanghai, China, in 2007 and 2009, respectively. She is currently pursuing her Ph.D. degree at Network Coding and Transmission Laboratory, Shanghai Jiao Tong University, Shanghai, China. Her current research interests include wireless network coding and cooperative communications.

Jun Li (M'09) received Ph.D. degree in Electronic Engineering from Shanghai Jiao Tong University, Shanghai, P. R. China in 2009. From January 2009 to June 2009, he worked in the Department of Research and Innovation, Alcatel Lucent Shanghai Bell as a Research Scientist. From June 2009 to April 2012, he was a Postdoctoral Fellow at the School of Electrical Engineering and Telecommunications, the University of New South Wales, Australia. From April 2012 to now, he is a Research Fellow at the School of Electrical Engineering, the University of Sydney, Australia. He served as the Technical Program Committee member for several international conferences such as APCC2009, APCC2010, VTC2011 (Spring), ICC2011, TENCON2012, APCC2013, VTC2014 (Fall), and ICC2014. His research interests include network information theory, channel coding theory, wireless network coding and cooperative communications.

Wen Chen (M'03CSM'11) received the B.S. and M.S. degrees from Wuhan University, China, in 1990 and 1993, respectively, and the Ph.D. degree from the University of Electro-Communications, Tokyo, Japan, in 1999. He was a researcher of Japan Society for the Promotion of Sciences (JSPS) from 1999 through 2001. In 2001, he joined the University of Alberta, Canada, starting as a Postdoctoral Fellow with the Information Research Laboratory and continuing as a Research Associate in the Department of Electrical and Computer Engineering. Since 2006, he has been a Full Professor in the Department of Electronic Engineering, Shanghai Jiao Tong University, China, where he is also the Director of the Institute for Signal Processing and Systems. His interests cover network coding, cooperative communications, cognitive radio, and MIMO-OFDM systems.

Hang Su received both BS and MS degrees in electronic engineering from Shanghai Jiao Tong University, Shanghai, China in 2007 and 2009, respectively. He is currently pursuing a Ph.D. degree at the Institute of Image Communication and Information Processing, Shanghai Jiaotong University, Shanghai, China. His current research interests include multimedia communication, computer vision and machine learning.

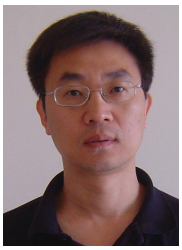

Zihuai Lin received the Ph.D. degree in Electrical Engineering from Chalmers University of Technology, Sweden, in 2006. Prior to this he has held positions at Ericsson Research, Stockholm, Sweden. Following Ph.D. graduation, he worked as a Research Associate Professor at Aalborg University, Denmark and currently as a senior lecturer at the School of Electrical and Information Engineering, the University of Sydney, Australia. His research interests include source/channel/network coding, coded modulation, MIMO, OFDMA, SC-FDMA, radio resource management, cooperative communications, HetNets etc.

Branka Vucetic (F?03) received the B.S.E.E., M.S.E.E., and Ph.D. degrees in electrical engineering, from the University of Belgrade, Belgrade, Yugoslavia, in 1972, 1978, and 1982, respectively. She currently holds the Peter Nicol Russel Chair of Telecommunications Engineering at the University of Sydney. She is an internationally recognized expert in wireless communications and coding and has been elected to the IEEE Fellow grade for her research contributions in channel coding and its applications in wireless communications. Her research has involved collaborations with industry and government organizations in Australia and several other countries.